



Universidad Autónoma
de Madrid

Biblos-e Archivo
Repositorio Institucional UAM

Repositorio Institucional de la Universidad Autónoma de Madrid
<https://repositorio.uam.es>

Esta es la **versión de autor** del artículo publicado en:
This is an **author produced version** of a paper published in:

Journal of Cosmology and Astroparticle Physics 2021.3 (2021): 090

DOI: <https://doi.org/10.1088/1475-7516/2021/03/090>

Copyright: © 2021 IOP Publishing Ltd and Sissa Medialab

El acceso a la versión del editor puede requerir la suscripción del recurso
Access to the published version may require subscription

Production of Thermal Axions across the ElectroWeak Phase Transition

Fernando Arias-Aragón^{a,b)} ^{*}, Francesco D'Eramo^{c,d)} [†],
Ricardo Z. Ferreira^{e,f)} [‡], Luca Merlo^{a,b)} [§], and Alessio Notari^{g)} [¶]

^{a)} *Instituto de Física Teórica UAM/CSIC, Calle Nicolás Cabrera 13-15, Cantoblanco E-28049 Madrid, Spain*

^{b)} *Departamento de Física Teórica, Universidad Autónoma de Madrid, Cantoblanco E-28049 Madrid, Spain*

^{c)} *Dipartimento di Fisica ed Astronomia, Università di Padova, Via Marzolo 8, 35131 Padova, Italy*

^{d)} *INFN, Sezione di Padova, Via Marzolo 8, 35131 Padova, Italy*

^{e)} *Nordita, KTH Royal Institute of Technology and Stockholm University,
Roslagstullsbacken 23, SE-106 91 Stockholm, Sweden*

^{f)} *Institut de Física d'Altes Energies (IFAE) and The Barcelona Institute of Science and Technology (BIST),
Campus UAB, 08193 Bellaterra, Barcelona*

^{g)} *Departament de Física Quàntica i Astrofísica & Institut de Ciències del Cosmos (ICCUB),
Universitat de Barcelona, Martí i Franquès 1, 08028 Barcelona, Spain*

Abstract

Light axions can potentially leave a cosmic background, just like neutrinos. We complete the study of thermal axion production across the electroweak scale by providing a smooth and continuous treatment through the two phases. Focusing on both flavor conserving and violating couplings to third generation quarks, we compute the amount of axions produced via scatterings and decays of thermal bath particles. We perform a model independent analysis in terms of axion effective couplings, and we also make predictions for specific microscopic QCD axion scenarios. This observable effect, parameterized as it is conventional by an effective number of additional neutrinos, is above the 1σ sensitivity of future CMB-S4 surveys. Moreover, if one assumes no large hierarchies among dimensionless axion couplings to standard model particles, future axion helioscopes will provide a complementary probe for the parameter region we study.

^{*}E-mail: fernando.arias@uam.es

[†]E-mail: francesco.deramo@pd.infn.it

[‡]E-mail: ricardo.zambujal@su.se

[§]E-mail: luca.merlo@uam.es

[¶]E-mail: notari@fqa.ub.edu

Contents

1	Introduction	1
2	Axion Effective Interactions	4
3	Axion Production Processes	6
3.1	Cross sections	6
3.2	Decay widths	10
4	Observable Consequences and Results	11
4.1	Model Independent results	13
4.2	UV Complete Models	17
5	Conclusions	20
A	Operator basis for axion couplings to quarks	21
B	Cross sections below the EWPT	22
C	Bounds on axion couplings	24
D	Approaching the QCDPT	26

1 Introduction

Understanding the absence of CP violation by strong interactions, an issue known as the strong CP problem, is a serious challenge for the Standard Model (SM) of particle physics. This remarkable invariance is unexpected since there are two potential sources of CP violation in the QCD Lagrangian,

$$\mathcal{L}_{\text{QCD}} \supset \frac{\alpha_s}{8\pi} \theta G_{\mu\nu}^a \tilde{G}^{a\mu\nu} - \left[\sum_{ij} \left(\overline{q_{Li}} M_{ij} q_{Rj} + \text{h.c.} \right) \right] \quad (1.1)$$

Here, $\alpha_s = g_s^2/(4\pi)$ is the QCD fine structure constant, $q_{L,Ri}$ are the quarks fields with i a flavor index, $G_{\mu\nu}^a$ and $\tilde{G}^{a\mu\nu} = \epsilon^{\mu\nu\rho\sigma} G_{\rho\sigma}^a/2$ are the QCD field strength tensor and its dual, respectively. An overall phase in the quark mass matrix M_{ij} , $\arg(\det(M)) \neq 0$, provides an additional source of CP violation in the quark sector beyond the CKM phase. One can transfer the full amount of CP violation on the first operator with θ replaced by $\bar{\theta} \equiv \theta - \arg(\det(M))$, and the non observation of a neutron electric dipole moment puts the spectacular bound $\bar{\theta} \leq 1.3 \times 10^{-10}$ [1,2].

An elegant solution was proposed in the late 70's by Peccei and Quinn (PQ) [3,4]. They introduced a new Abelian symmetry $U(1)_{\text{PQ}}$, dubbed PQ symmetry, with two key features: anomalous with respect to the $SU(3)_c$ color gauge group, and spontaneously

broken at a scale f_a . The low-energy residual is a pseudo-Nambu-Goldstone boson (PNGB) a , known as the axion [5, 6], which acquires the anomalous coupling to gluons

$$\mathcal{L}_{\text{axion}} \supset \frac{\alpha_s}{8\pi} \frac{a}{f_a} G_{\mu\nu}^a \tilde{G}^{a\mu\nu}. \quad (1.2)$$

This equation, valid before the axion mixes with the η and π^0 mesons, defines f_a . Non-perturbative QCD effects generate an axion potential, and a theorem due to Vafa and Witten [7] ensures a CP conserving minimum. Moreover, the axion potential leads to the general relation for its mass [8, 9]

$$m_a = 5.70(6)(4) \mu\text{eV} \left(\frac{10^{12} \text{ GeV}}{f_a} \right) \left(\cdot \right) \quad (1.3)$$

The first error is due to the uncertainty in the up-down quark mass ratio whereas the second one is due to uncertainties in low energy couplings. Axion couplings are proportional to $1/f_a$, and f_a is bound by astrophysical and terrestrial searches [10–14], spanning the range $f_a \gtrsim 10^6 - 10^9$ GeV: the axion must be light and weakly-coupled (scenario dubbed as the invisible axion [15–18]). The energy density stored in the axion field can account for dark matter (DM) for values of f_a allowed experimentally [19].

The focus of this work is on a different and distinct cosmological imprint: scattering and/or decay of particles in the primordial plasma produce relativistic axions [20, 21]. Current bounds on f_a implies that m_a must be roughly below the eV scale. Axions produced at early times are still relativistic at matter-radiation equality and, for $m_a \ll \mathcal{O}(0.1)$ eV as we consider by neglecting the axion mass, also around recombination. In this case, they would manifest themselves as an additional contribution to the amount of radiation at the time of CMB formation. Upcoming CMB-S4 surveys [22, 23] will improve bounds on this quantity, historically parameterized as an effective number of neutrino species N_{eff} , and can potentially discover a deviation from the SM. The forecasted sensitivity allows to detect the effects of a relativistic species which decoupled at high temperatures, as high as the ElectroWeak Phase Transition (EWPT), making this a new probe of high-energy physics. Motivated by forthcoming data, recent works revisited axion production through various channels and the resulting prediction for N_{eff} [24–28]. Furthermore, this could be a complementary probe of the axion interpretation for the excess in the number of electron recoil events observed recently by the XENON1T experiment [29] as highlighted by Ref. [30].

There are, broadly speaking, two classes of axion interactions with visible matter

$$\mathcal{L}_{\text{axion-int}} \supset \frac{1}{f_a} \left[c_X \frac{\alpha_X}{8\pi} X^{a\mu\nu} \tilde{X}_{\mu\nu}^a + \partial_\mu a c_\psi \bar{\psi} \gamma^\mu \psi \right] \left(\cdot \right) \quad (1.4)$$

Operators with gauge bosons $X = \{G, W, B\}$, present if the PQ symmetry is anomalous under the associated gauge group, are suppressed by a loop factor. We need a coupling to gluons in order to solve the strong CP problem, and we set $c_G = 1$ consistently with Eq. (1.2). Anomalies under the electroweak group are possible but not mandatory. We consider the high-energy theory where SM fermions, $\psi = \{Q_L, u_R, d_R, L_L, e_R\}$, have well defined gauge quantum numbers and their interactions with the axion preserve

the shift symmetry $a \rightarrow a + \text{const.}$ Other dimension 5 interactions can be redefined away as explained later in the text.

Axion production is efficient when the interaction rate exceeds the Hubble rate H . The latter, assuming an early universe dominated by radiation with temperature T , scales as $H \propto T^2/M_{\text{Pl}}$. Hot axions can be produced either via scatterings or decays. Interactions with gauge bosons, the first kind in Eq. (1.4), cannot mediate decays. Coupling to SM fermions, the second kind in Eq. (1.4), could in principle be responsible for production via decays if the fermion bilinear couples fields belonging to different generations. In other words, we need flavor violation in order to have production via unsuppressed tree-level bath particles decays to axions.

Regardless of the production details, the highest value for N_{eff} is reached when axions achieve thermalization with the thermal bath. The resulting abundance in this case depends only on the plasma temperature when they lose thermal contact, and its value is suppressed by the total number of the entropic degrees of freedom g_{*s} at decoupling. If this happens above the EWPT then the resulting N_{eff} is barely within the reach of future surveys [24].

Rates for scattering mediated by interactions with SM gauge bosons scale at high temperatures as $\Gamma_X \simeq \alpha_X^3 T^3/f_a^2$, and these processes are never in thermal equilibrium at the EWPT for $f_a \gtrsim \mathcal{O}(10^8)$ GeV [21, 25]. If axions never thermalize, the prediction for N_{eff} is sensitive to the initial abundance that is presumably set at the stage of reheating after inflation; an accurate calculation requires a treatment of thermal effects at high temperature [25]. Either way, the associated N_{eff} is at the edge of what we can test.

Once considering interactions with fermions, for flavor conserving couplings, the only way to produce hot axions is via scattering. We consider $2 \rightarrow 2$ collisions, and these processes always involve two SM fermions and one SM boson besides the axion itself.

At temperatures above the EWPT, we have two options for the SM boson involved. On the one hand, it can be any of the four real component of the Higgs doublet H ¹ and the scattering rate in this case scales as $\Gamma_{\psi/H} \simeq c_\psi^2 y_\psi^2 T^3/f_a^2$ [25] with y_ψ the SM fermion Yukawa coupling. For heavy SM fermions, this is larger by a factor $c_\psi^2 y_\psi^2/\alpha_X^3$ compared to scattering mediated by the axion-gauge boson vertex. On the other hand, it can be a transverse gauge boson. The scattering rate in this case is proportional to the mass of the fermion, since there is a chirality flip needed in the process, and this contribution is vanishing because all fermions are massless above the EWPT.

The SM boson involved in the scattering with fermions can be a gauge field only below the EWPT. The associated rate scales as $\Gamma_{\psi/X} \simeq \alpha_X c_\psi^2 m_\psi^2 T/f_a^2$ for temperatures above the fermion mass, where m_ψ^2 reflects the fermion chirality flip mentioned in the paragraph above, and it is exponentially suppressed at lower temperatures. In this case, at temperatures above the fermion mass, the scattering rate grows with the temperature slower than the Hubble rate and thus axion production is saturated when the ratio between interaction and expansion rates is maximal. This happens at temperatures around the fermion mass, and such a ratio is approximately $\Gamma_{\psi/X}/H|_{T=m_\psi} \approx$

¹Namely the Higgs boson and what would become the longitudinal components of the weak gauge bosons below the EWPT scale.

$\alpha_X c_\psi m_\psi M_{Pl}/f_a^2$. If this quantity is larger than $\mathcal{O}(1)$ thermalization is achieved, and the final abundance is not affected by our ignorance about the thermal history (assuming reheating above the weak scale) and possible new degrees of freedom and/or interactions at high energy.

Decays of SM fermions provide an additional axion production channel, often the dominant one, if we have flavor violating couplings. The interaction rate is given by the rest frame width of the decaying fermion times a Lorentz dilation factor accounting for the bath kinetic energy, and it scales as $\Gamma_\psi \simeq c_\psi^2 m_\psi^4/(f_a^2 T)$. Axion production is saturated at temperatures around the fermion mass also in this case, and we achieve thermalization if the condition $\Gamma_\psi/H|_{T=m_\psi} \approx c_\psi^2 m_\psi M_{Pl}/f_a^2$ is satisfied.

After this comparison among different production channels, we decide to focus on axion production mediated by its interactions with SM fermions. We analyze processes with third generation quarks. Production via leptons has been studied in Ref. [28], and such an axion abundance can alleviate the current tension in the measurement of the Hubble parameter [31]. A full calculation via the first two quark generations would require a careful treatment of the QCD phase transition (QCDPT) and it is beyond the scope of this work. Previous studies have considered production well above [25] and well below [27] the EWPT. We improve earlier treatments by providing a continuous and smooth prediction for N_{eff} across the EWPT.

We introduce the theoretical framework in Sec. 2, and we describe axion effective interactions considering both flavor conserving and violating couplings. We collect in Sec. 3 all the processes contributing to axion production, and we provide explicit expressions for cross sections and decay widths. In particular, we compute cross section both above and below the EWPT and we match them at this threshold. We feed Boltzmann equations with these quantities and we solve them numerically, presenting predictions for N_{eff} as a function of the fermion couplings in Sec. 4. We consider both effective interactions as well as explicit UV constructions leading to flavor conserving couplings. Remarkably, our predictions are within the reach of future CMB surveys inside the low- f_a part of the experimentally allowed region. It is to be noted that, as we discuss in our conclusions in Sec. 5, in the absence of no big hierarchy in the dimensionless coefficient describing the coupling to photons, we find that the same parameter space will be probed by future terrestrial searches.

2 Axion Effective Interactions

Axion interactions with SM fields can be written compactly as follows

$$\mathcal{L}^{(a)} = \mathcal{L}_{\text{gauge}}^{(a)} + \mathcal{L}_{\text{matter}}^{(a)} , \quad (2.1)$$

where $\mathcal{L}_{\text{gauge}}^{(a)}$ and $\mathcal{L}_{\text{matter}}^{(a)}$ describe couplings with SM gauge bosons and matter fields, respectively. The entire focus of our work is on axion couplings with SM quarks. However, there are usually relations among different axion interactions once one considers UV complete models. For this reason, we provide an overview of all axion couplings

and we summarize their bounds in App. C in order to visualize which parameter space region is not excluded experimentally.

The axion has anomalous couplings to gauge bosons

$$\mathcal{L}_{\text{gauge}}^{(a)} = -\frac{a}{f_a} \left(\frac{\alpha_s}{8\pi} G_{\mu\nu}^a \tilde{G}^{a\mu\nu} + c_W \frac{\alpha_W}{8\pi} W_{\mu\nu}^a \tilde{W}^{a\mu\nu} + c_B \frac{\alpha_Y}{8\pi} B_{\mu\nu} \tilde{B}^{\mu\nu} \right) \quad (2.2)$$

where \tilde{W} and \tilde{B} are defined as \tilde{G} below Eq. (1.2). These operators should be interpreted as the effects of the presence of any fermion that couples to the axion and are associated to quantum level contributions. As already mentioned in the Introduction, the gluon term does not present any free coefficient, in contrast with the EW terms, in order to match with the traditional definition of f_a . Once we integrate-out weak scale states and heavy quarks, the Lagrangian contains axion couplings to only gluons and photons

$$\mathcal{L}_{\text{gauge}}^{(a)} \supset -\frac{a}{f_a} \left(\frac{\alpha_s}{8\pi} G_{\mu\nu}^a \tilde{G}^{a\mu\nu} + c_{a\gamma\gamma} \frac{\alpha_{\text{em}}}{8\pi} F_{\mu\nu} \tilde{F}^{\mu\nu} \right) \quad (2.3)$$

where $c_{a\gamma\gamma} = c_B \cos^2 \theta_W + c_W \sin^2 \theta_W$, being θ_W the Weinberg angle. This expression is valid above the scale where strong interactions confine and therefore before the axion mixes with the η and π^0 mesons. However, experimental searches probe the axion-photon coupling at much lower energy scales and therefore this mixing is to be taken into account. We define this coupling as follows:

$$g_{a\gamma\gamma} \equiv \frac{\alpha_{\text{em}}}{2\pi} \frac{1}{f_a} \left(c_{a\gamma\gamma} - 1.92(4) \right), \quad (2.4)$$

where the second term in the parenthesis is the model-independent contribution arising from the above mentioned axion mixing with the η' and π^0 mesons [9, 32–35].

We present matter couplings for the case of quarks, the discussion is analogous if we consider leptons. Axion couplings to quarks can be expressed in different field basis and physical results cannot depend on such a choice. However, the statement that the axion couples without flavor violation is not true in an arbitrary basis. We specify axion couplings to quarks in the “primed basis” defined in App. A where the fields appearing in the Lagrangian are the $SU(2)_L$ quark doublets Q'_L , and the $SU(2)_L$ singlets u'_R and d'_R , and where Yukawa interactions take the form of Eq. (A.4).

We distinguish between two cases, and we begin from flavor conserving axion-quark interactions

$$\mathcal{L}_{\text{matter}}^{(a)} \supset \mathcal{L}_{\partial\text{-F.C.}}^{(a)} = \frac{\partial_\mu a}{f_a} \sum_{i=1}^3 \left(c_Q \overline{Q'_{Li}} \gamma^\mu Q'_{Li} + c_u \overline{u'_{Ri}} \gamma^\mu u'_{Ri} + c_d \overline{d'_{Ri}} \gamma^\mu d'_{Ri} \right), \quad (2.5)$$

where the free coefficients $\{c_Q, c_u, c_d\}$ are typically of the same order of magnitude. The universality of quark-axion couplings guarantees that no flavor-changing interactions arise when moving to the quark mass basis. We can see it explicitly after performing the rotation to get mass eigenstates given in Eq. (A.5), the unitarity of the CKM matrix ensures that in the mass eigenbasis the fermion couplings are still flavor conserving.

The most general flavor violating part of the Lagrangian above the EWPT can be written in an analogous way to the flavor conserving one as follows

$$\mathcal{L}_{\text{matter}}^{(a)} \supset \mathcal{L}_{\text{F.V.}}^{(a)} = \frac{\partial_\mu a}{f_a} \sum_{i,j} \left(c_Q^{(ij)} \overline{Q}_{Li} \gamma^\mu Q'_{Lj} + c_u^{(ij)} \overline{u}'_{Ri} \gamma^\mu u'_{Rj} + c_d^{(ij)} \overline{d}'_{Ri} \gamma^\mu d'_{Rj} \right), \quad (2.6)$$

where the matrices of coefficients $\{c_Q^{(ij)}, c_u^{(ij)}, c_d^{(ij)}\}$ have a generic structure in flavor space. Unless we tune the entries of these matrices consistently with CKM factors, couplings are still flavor off-diagonal once we go to the mass eigenstate basis.

We complete this overview on axion couplings by discussing the remaining options. The case of coupling to leptons is analogous, and Ref. [28] exploited their cosmological consequences. Besides interactions with leptons, no other matter couplings can be present in the Lagrangian as an independent operator. The Higgs-axion interaction

$$i \frac{\partial_\mu a}{f_a} H^\dagger \overleftrightarrow{D}^\mu H, \quad (2.7)$$

where $H^\dagger \overleftrightarrow{D}^\mu H \equiv H^\dagger (D^\mu H) - (D^\mu H)^\dagger H$ is redundant at lowest order in $1/f_a$ as can be shown via a field redefinition. Moreover, axion couplings to pseudo-scalar fermion currents such as

$$i \frac{a}{f_a} \overline{Q}'_L H d'_R, \quad (2.8)$$

can be proved to be also redundant.

3 Axion Production Processes

Multiple processes contribute to the production of hot axions in the early universe, and we list all of them in this section. Binary scatterings control production for the flavor conserving case since decays are loop and CKM suppressed. We provide the associated scattering cross sections above and below the weak scale, and we match our results across the EWPT. If axion couplings are flavor violating then tree-level decays dominate the production rate. We give here the associated decay widths.

Axion couplings to quarks are a crucial ingredient for our calculations, and we remark how we define them in the “primed basis” where the SM Yukawa interactions take the form in Eq. (A.4). One of our main goals is to provide a smooth treatment of production through the EWPT, hence it is convenient to work in the mass eigenbasis.

3.1 Cross sections

We start from flavor conserving axion couplings defined in Eq. (2.5) and quantified by the scale f_a and the three dimensionless coefficients $\{c_Q, c_u, c_d\}$. As it turns out, scattering cross sections depend only on two linear combinations of them. This can be

checked through explicit calculations or via a change of basis. We perform the following rotations where we redefine quark fields by an axion-dependent phase

$$Q'_{Li} \rightarrow e^{ic_Q \frac{a}{f_a}} Q'_{Li}, \quad u'_{Rj} \rightarrow e^{ic_u \frac{a}{f_a}} u'_{Rj}, \quad d'_{Rj} \rightarrow e^{ic_d \frac{a}{f_a}} d'_{Rj}. \quad (3.1)$$

These chiral rotations modify several couplings in the Lagrangian. First, they are anomalous and the dimensionless coefficients of axion couplings to gauge bosons in Eq. (2.3) are affected; as already stated above we do not consider these interactions for our processes and we do not need to worry about this effect. Second, we generate new axion derivative couplings equal and opposite to the ones in Eq. (2.5) once we plug the new quark fields defined above in the kinetic terms. Thus axion derivative couplings are not present anymore in the Lagrangian. Third, and crucially for us, the axion field appears in the Yukawa interactions after we plug these field redefinitions into the SM Yukawa Lagrangian, whose explicit expression is given in Eq. (A.4), and we find

$$-\mathcal{L}_{Y\text{-F.C.}}^{(a)} = e^{i(c_u - c_Q) \frac{a}{f_a}} \overline{Q'_L} \tilde{H} \hat{Y}^u u'_R + e^{i(c_d - c_Q) \frac{a}{f_a}} \overline{Q'_L} H V_{\text{CKM}} \hat{Y}^d d'_R + \text{h.c.} \quad (3.2)$$

As anticipated, although there are three different couplings in the theory only two linear combinations of them can appear in scattering amplitudes

$$c_t \equiv -c_Q + c_u, \quad (3.3)$$

$$c_b \equiv -c_Q + c_d. \quad (3.4)$$

We label them with the top and bottom quark because we only focus on the third quark generation as explained in the Introduction. The hatted matrices $\hat{Y}^{u,d}$ are diagonal in flavor space, and axion interactions are flavor conserving once we switch to the mass eigenbasis via the rotations given in Eq. (A.5).

Scattering cross sections above EWPT

We focus on third generation quarks $\{t_L, b_L, t_R, b_R\} = \{u_{L3}, d_{L3}, u_{R3}, d_{R3}\}$ where we assign new names to left- and right-handed fields. In order to write explicitly their interactions, we parameterize the complex components of the Higgs doublet as follows

$$H = \begin{pmatrix} \chi_+ \\ \chi_0 \end{pmatrix}, \quad \tilde{H} \equiv i\sigma_2 (H^\dagger)^T = \begin{pmatrix} \chi_0^c \\ -\chi_- \end{pmatrix}, \quad (3.5)$$

where we define $\chi_- \equiv \chi_+^\dagger$ and $\chi_0^c \equiv \chi_0^\dagger$. Once we focus on third generation quarks and we consider the Lagrangian in Eq. (3.2) in the mass eigenbasis, namely without the CKM matrix, we find the following axion interactions

$$-\mathcal{L}_{Y\text{-F.C.}}^{(a)} = y_t e^{ic_t \frac{a}{f_a}} [\chi_0^c \bar{t}_L t_R - \chi_- \bar{b}_L t_R] + y_b e^{ic_b \frac{a}{f_a}} [\chi_+ \bar{t}_L b_R + \chi_0^c \bar{b}_L b_R] + y_t e^{-ic_t \frac{a}{f_a}} [\chi_0 \bar{t}_R t_L - \chi_+ \bar{t}_R b_L] + y_b e^{-ic_b \frac{a}{f_a}} [\chi_- \bar{b}_R t_L + \chi_0^c \bar{b}_R b_L]. \quad (3.6)$$

The processes we are interested in have only one axion field in the external legs, thus we can Taylor expand the exponential functions appearing in the above Lagrangian and only keep terms up to the first order.

Axion Production Above EWSB		
Process	CP Conjugate	$\sigma_{ij \rightarrow ka} \times 64\pi f_a^2$
$t\bar{t} \rightarrow \chi_0 a$	$t\bar{t} \rightarrow \chi_0^c a$	$c_t^2 y_t^2$
$b\bar{b} \rightarrow \chi_0 a$	$b\bar{b} \rightarrow \chi_0^c a$	$c_b^2 y_b^2$
$t\bar{b} \rightarrow \chi_+ a$	$b\bar{t} \rightarrow \chi_- a$	$c_t^2 y_t^2 + c_b^2 y_b^2$
$t\chi_0 \rightarrow ta$	$\bar{t}\chi_0^c \rightarrow \bar{t}a$	$c_t^2 y_t^2$
$t\chi_0^c \rightarrow ta$	$\bar{t}\chi_0 \rightarrow \bar{t}a$	$c_t^2 y_t^2$
$b\chi_0 \rightarrow ba$	$\bar{b}\chi_0^c \rightarrow \bar{b}a$	$c_b^2 y_b^2$
$b\chi_0^c \rightarrow ba$	$\bar{b}\chi_0 \rightarrow \bar{b}a$	$c_b^2 y_b^2$
$t\chi_- \rightarrow ba$	$\bar{t}\chi_+ \rightarrow \bar{b}a$	$c_t^2 y_t^2 + c_b^2 y_b^2$
$b\chi_+ \rightarrow ta$	$\bar{b}\chi_- \rightarrow \bar{t}a$	$c_t^2 y_t^2 + c_b^2 y_b^2$

Table 1: Scatterings producing axions above the EWPT. In the first two columns we list the process and its CP conjugate. They have the same cross section, listed on the third column.

In the unbroken electroweak phase, the Higgs vev is vanishing and all particles are massless. We want to consider processes producing one axion particle in the final state thus the most general binary collisions involve two fermions fields. The other boson in the process can be either a component of the Higgs doublet or a SM gauge boson. However, if we look at the axion interactions in Eq. (3.6) we see that only the former is possible. There is no $2 \rightarrow 2$ scattering with SM gauge bosons; this is manifest in the basis we choose to describe axion couplings. Alternatively, if we insisted on working in the basis where axion is derivatively coupled to SM fermions the amplitude for a $2 \rightarrow 2$ is vanishing as it requires a fermion chirality flip that is not possible in the absence of a mass term for the fermion itself.

We only have processes with the components of the Higgs doublet in Eq. (3.5). The two fermions in the scattering can be either both in the initial state or one in the initial state and the other one in the final state. We classify all possible cases according to where fermions appear. If we consider the first case, we have fermion/antifermion annihilations producing an axion and any of the components of the complex Higgs doublet. The possible processes are listed in the first block of Tab. 1; we show the associated CP conjugate on the same row, and we correctly account for both in our numerical analysis. Another possibility is to have just one fermion in the initial state, and the other particle would be a component of the Higgs doublet. The associated processes are listed in the second block of Tab. 1. For each process we also provide the scattering cross section. Our contribution proportional to y_t^2 agrees with what was found in Ref. [25].

Scattering cross sections below EWPT

Once the electroweak symmetry is broken, the Higgs field gets a vacuum expectation value (vev) which gives mass to SM particles. We work in unitarity gauge where the

Axion Production Below EWSB					
Process	CP Conjugate	$\sigma_{ij \rightarrow ka}$	Process	CP Conjugate	$\sigma_{ij \rightarrow ka}$
$t\bar{t} \rightarrow ga$	Same	Eq. (B.1)	$tg \rightarrow ta$	$\bar{t}g \rightarrow \bar{t}a$	Eq. (B.6)
$b\bar{b} \rightarrow ga$	Same		$bg \rightarrow ba$	$\bar{b}g \rightarrow \bar{b}a$	
$t\bar{t} \rightarrow ha$	Same	Eq. (B.2)	$th \rightarrow ta$	$\bar{t}h \rightarrow \bar{t}a$	Eq. (B.7)
$b\bar{b} \rightarrow ha$	Same		$bh \rightarrow ba$	$\bar{b}h \rightarrow \bar{b}a$	
$t\bar{t} \rightarrow Za$	Same	Eq. (B.3)	$tZ \rightarrow ta$	$\bar{t}Z \rightarrow \bar{t}a$	Eq. (B.8)
$b\bar{b} \rightarrow Za$	Same	Eq. (B.4)	$bZ \rightarrow ba$	$\bar{b}Z \rightarrow \bar{b}a$	Eq. (B.9)
$t\bar{b} \rightarrow W^+a$	$b\bar{t} \rightarrow W^-a$	Eq. (B.5)	$tW^- \rightarrow ba$	$\bar{t}W^+ \rightarrow \bar{b}a$	Eq. (B.10)
			$bW^+ \rightarrow ta$	$\bar{b}W^- \rightarrow \bar{t}a$	Eq. (B.11)

Table 2: Scatterings producing axions below the EWPT. We give the process (left column), the CP conjugate (central column) and the reference to the equation with the explicit analytical expression for the scattering cross section.

Higgs field is parameterized by the following field coordinates

$$H = \begin{pmatrix} 0 \\ \frac{v+h}{\sqrt{2}} \end{pmatrix}, \quad \tilde{H} \equiv i\sigma_2(H^\dagger)^T = \begin{pmatrix} \frac{v+h}{\sqrt{2}} \\ 0 \end{pmatrix}, \quad (3.7)$$

where v and h are the vev and the physical Higgs boson, respectively. In such a gauge, the three remaining (Goldstone) components of the Higgs doublet are eaten up by the massive Z and W bosons. The mass spectrum as a function of the Higgs vev results in

$$\{m_W, m_Z, m_h, m_f\} = \left\{ \frac{g}{2}, \frac{\sqrt{g^2 + g'^2}}{2}, \sqrt{\frac{\lambda}{2}}, \frac{y_f}{\sqrt{2}} \right\} v. \quad (3.8)$$

Here, g and g' are the $SU(2)_L$ and $U(1)_Y$ gauge couplings, respectively. The Higgs quartic coupling λ is normalized in such a way that the potential term is $\lambda(H^\dagger H)^2$.

We list in Tab. 2 all processes contributing to axion production in the phase where the electroweak symmetry is broken. As done already above, we provide also the CP conjugate process as well as the scattering cross section. The explicit expressions are too lengthy to be displayed directly in the table and we give their explicit analytical expressions in App. B.

Matching at the EWPT

We complete our discussion of production via scattering by showing how processes involving the four components of the Higgs doublet, three of which are the longitudinal components of the Z and W bosons below the EWPT, match at the point of electroweak symmetry breaking. For this reason, the Z and W components involved in the following processes are the longitudinal ones and will be denoted with an index L in the rest of this subsection. In the following, we will take the cross sections for the different processes, express all masses in terms of the Higgs vev and run towards $v \rightarrow 0$. The process that will match are shown in Tab. 3.

- *Neutral annihilations:* $t\bar{t} \rightarrow \chi_0 a, \quad t\bar{t} \rightarrow \chi_0^c a; \quad t\bar{t} \rightarrow h a, \quad t\bar{t} \rightarrow Z_L a.$

When considering the limit in which the Higgs vev vanishes, the cross sections below EWPT coincide exactly with those above, as expected:

$$\sigma_{t\bar{t} \rightarrow \chi_0 a} + \sigma_{t\bar{t} \rightarrow \chi_0^c a} = \sigma_{t\bar{t} \rightarrow h a} + \sigma_{t\bar{t} \rightarrow Z_L a} = \frac{c_t^2 y_t^2}{32\pi f_a^2}. \quad (3.9)$$

- *Neutral scatterings:* $t\chi_0 \rightarrow ta, \quad t\chi_0^c \rightarrow ta; \quad th \rightarrow ta, \quad tZ_L \rightarrow ta.$
 $\bar{t}\chi_0 \rightarrow \bar{t}a, \quad \bar{t}\chi_0^c \rightarrow \bar{t}a; \quad \bar{t}h \rightarrow \bar{t}a, \quad \bar{t}Z_L \rightarrow \bar{t}a.$

In this case, the matching can be expressed as:

$$\begin{aligned} \sigma_{t\chi_0 \rightarrow ta} + \sigma_{t\chi_0^c \rightarrow ta} &= \sigma_{th \rightarrow ta} + \sigma_{tZ_L \rightarrow ta} = \\ &= \sigma_{\bar{t}\chi_0 \rightarrow \bar{t}a} + \sigma_{\bar{t}\chi_0^c \rightarrow \bar{t}a} = \sigma_{\bar{t}h \rightarrow \bar{t}a} + \sigma_{\bar{t}Z_L \rightarrow \bar{t}a} = \frac{c_t^2 y_t^2}{32\pi f_a^2}, \end{aligned} \quad (3.10)$$

where the CP conjugates give indeed the same contribution.

- *Charged annihilations:* $t\bar{b} \rightarrow \chi_+ a, \quad b\bar{t} \rightarrow \chi_- a; \quad t\bar{b} \rightarrow W_L^+ a, \quad b\bar{t} \rightarrow W_L^- a.$

Analogously to the neutral case, the charged annihilations can be matched as:

$$\sigma_{t\bar{b} \rightarrow \chi_+ a} + \sigma_{b\bar{t} \rightarrow \chi_- a} = \sigma_{t\bar{b} \rightarrow W_L^+ a} + \sigma_{b\bar{t} \rightarrow W_L^- a} = \frac{c_t^2 y_t^2 + c_b^2 y_b^2}{32\pi f_a^2}. \quad (3.11)$$

- *Charged scatterings:* $t\chi_- \rightarrow ba, \quad b\chi_+ \rightarrow ta; \quad tW_L^- \rightarrow ba, \quad bW_L^+ \rightarrow ta.$
 $\bar{t}\chi_+ \rightarrow \bar{b}a, \quad \bar{b}\chi_- \rightarrow \bar{t}a; \quad \bar{t}W_L^+ \rightarrow \bar{b}a, \quad \bar{b}W_L^- \rightarrow \bar{t}a.$

Finally, these set of processes match their cross section as follows:

$$\begin{aligned} \sigma_{t\chi_- \rightarrow ba} + \sigma_{b\chi_+ \rightarrow ta} &= \sigma_{tW_L^- \rightarrow ba} + \sigma_{bW_L^+ \rightarrow ta} = \\ &= \sigma_{\bar{t}\chi_+ \rightarrow \bar{b}a} + \sigma_{\bar{b}\chi_- \rightarrow \bar{t}a} = \sigma_{\bar{t}W_L^+ \rightarrow \bar{b}a} + \sigma_{\bar{b}W_L^- \rightarrow \bar{t}a} = \frac{c_t^2 y_t^2 + c_b^2 y_b^2}{32\pi f_a^2}. \end{aligned} \quad (3.12)$$

3.2 Decay widths

The crucial ingredient for axion production via quark decays is the Lagrangian with flavor violating interactions whose explicit expression is given in Eq. (2.6). This channel is active only below the EWPT because it is kinematically forbidden at higher temperatures where all quarks are massless. For this reason, we find it convenient to rewrite it in terms of Dirac quark fields $u = (u_L \ u_R)$ and $d = (d_L \ d_R)$ in the mass eigenstate basis

$$\mathcal{L}_{\partial\text{-F.V.}}^{(a)} = \frac{\partial_\mu a}{f_a} \sum_{i,j} \left[\bar{u}_i \gamma^\mu \left(c_{V_u}^{(ij)} + c_{A_u}^{(ij)} \gamma_5 \right) u_j + \bar{d}_i \gamma^\mu \left(c_{V_d}^{(ij)} + c_{A_d}^{(ij)} \gamma_5 \right) d_j \right] \quad (3.13)$$

Processes Above EWPT	Processes Below EWPT
$t\bar{t} \rightarrow \chi_0 a + t\bar{t} \rightarrow \chi_0^c a$ $t\bar{b} \rightarrow \chi_+ a$ $b\bar{t} \rightarrow \chi_- a$ $t\chi_0 \rightarrow ta + t\chi_0^c \rightarrow ta$ $\bar{t}\chi_0 \rightarrow \bar{t}a + \bar{t}\chi_0^c \rightarrow \bar{t}a$ $t\chi_- \rightarrow ba$ $\bar{t}\chi_+ \rightarrow \bar{b}a$ $b\chi_+ \rightarrow ta$ $\bar{b}\chi_- \rightarrow \bar{t}a$	$t\bar{t} \rightarrow ha + t\bar{t} \rightarrow Z_L a$ $t\bar{b} \rightarrow W_L^+ a$ $b\bar{t} \rightarrow W_L^- a$ $th \rightarrow ta + tZ_L \rightarrow ta$ $\bar{t}h \rightarrow \bar{t}a + \bar{t}Z_L \rightarrow \bar{t}a$ $tW_L^- \rightarrow ba$ $\bar{t}W_L^+ \rightarrow \bar{b}a$ $bW_L^+ \rightarrow ta$ $\bar{b}W_L^- \rightarrow \bar{t}a$

Table 3: Scatterings producing axions involving the Higgs doublet above and below the EWPT. We consider the four components of the Higgs doublet above, and we work in unitary gauge below with the Higgs boson h and the longitudinal components Z_L and W_L of the weak bosons.

Axion Production Above EWSB		
Process	CP Conjugate	$\Gamma_{i \rightarrow ja} \times 16\pi f_a^2 / m_i^3$
$t \rightarrow ca$	$\bar{t} \rightarrow \bar{c}a$	$c_{V_u}^{(tc)^2} + c_{A_u}^{(tc)^2}$
$t \rightarrow ua$	$\bar{t} \rightarrow \bar{u}a$	$c_{V_u}^{(tu)^2} + c_{A_u}^{(tu)^2}$
$b \rightarrow sa$	$\bar{b} \rightarrow \bar{s}a$	$c_{V_d}^{(bs)^2} + c_{A_d}^{(bs)^2}$
$b \rightarrow da$	$\bar{b} \rightarrow \bar{d}a$	$c_{V_d}^{(bd)^2} + c_{A_d}^{(bd)^2}$

Table 4: Quark decays producing axions. In the first two columns we list the process and its CP conjugate, and they both have the same decay widths listed on the third column.

where we identify the following combinations

$$\left\{ c_{V_u}^{(ij)}, c_{A_u}^{(ij)}, c_{V_d}^{(ij)}, c_{A_d}^{(ij)} \right\} = \frac{1}{2} \times \left\{ q_u^{(ij)} + c_Q^{(ij)}, c_u^{(ij)} - c_Q^{(ij)}, c_d^{(ij)} + c_Q^{(ij)}, c_d^{(ij)} - c_Q^{(ij)} \right\} \quad (3.14)$$

The decay process $q_i \rightarrow q_j a$ and its CP conjugate $\bar{q}_i \rightarrow \bar{q}_j a$, which can happen for both up- and down-type quarks, have the following decay width

$$\Gamma_{q_i \rightarrow q_j a} = \frac{m_i^3}{16\pi f_a^2} \left(q_{V_q}^{(ij)^2} + c_{A_q}^{(ij)^2} \right) \left(1 - \frac{m_j^2}{m_i^2} \right)^3. \quad (3.15)$$

Here, the ratio $\frac{m_j}{m_i}$ can safely be neglected as it leads to non observable changes in ΔN_{eff} . The decays relevant to our analysis and their CP conjugates are displayed in Tab. 4 with their corresponding decay widths.

4 Observable Consequences and Results

The physical observable of interest in our work is the effective number of neutrinos N_{eff} induced by hot axions. Big bang nucleosynthesis [36] and CMB experiments [22, 37]

probe this quantity, and we focus on the latter case as it is the most sensitive. Here, we first review briefly how to compute N_{eff} from a given axion production source and then we quantify the N_{eff} generated from all processes analyzed in the previous section.

The effective number of neutrinos is related to the radiation energy density ρ_{rad} as

$$\rho_{\text{rad}} = \rho_{\gamma} \left[1 + \frac{7}{8} \left(\frac{T_{\nu}}{T_{\gamma}} \right)^4 N_{\text{eff}} \right], \quad (4.1)$$

where ρ_{γ} is the photon energy density. Any relativistic particle with a non-negligible energy density, like neutrinos or axions, will contribute to N_{eff} . In particular, we are interested in deviations from the ΛCDM value

$$\Delta N_{\text{eff}} \equiv N_{\text{eff}} - N_{\text{eff}}^{\Lambda\text{CDM}} = \frac{8}{7} \left(\frac{11}{4} \right)^{4/3} \frac{\rho_a}{\rho_{\gamma}}, \quad (4.2)$$

with $N_{\text{eff}}^{\Lambda\text{CDM}} = 3.046$ and ρ_a is the axion energy density.

In order to connect with the numerical solutions of Boltzmann equations, we find it convenient to rewrite ΔN_{eff} in terms of the comoving axion abundance $Y_a \equiv n_a/s$. Here, n_a is the axion number density and $s = 2\pi^2 g_{*s} T^3/45$ is the entropy density with g_{*s} the number of entropic degrees of freedom. The photon energy density can also be expressed as follows

$$\rho_{\gamma} = 2 \times \frac{\pi^2}{30} \left(\frac{45 s}{2\pi^2 g_{*s}} \right)^{4/3}, \quad (4.3)$$

whereas the axion energy density is related to the number density via

$$\rho_a = \frac{\pi^2}{30} \left(\frac{\pi^2 n_a}{\zeta(3)} \right)^{4/3}. \quad (4.4)$$

We combine these two equations and find

$$\Delta N_{\text{eff}} \simeq 74.85 Y_a^{4/3}, \quad (4.5)$$

where we used the value of g_{*s} at recombination $g_{*s} = 43/11$.

We determine the asymptotic value of the axion number density by solving the associated Boltzmann equation. The differential equation describing how the axion number density evolves with time reads

$$\frac{d}{dt} n_a + 3H n_a = \left[\sum_S \bar{\Gamma}_S + \sum_D \bar{\Gamma}_D \right] (n_a^{\text{eq}} - n_a). \quad (4.6)$$

Here, H is the Hubble parameter quantifying the expansion rate of the universe and the superscript “eq” for number density denotes expressions valid when particles are in thermal equilibrium. The two terms on the right hand side denote, respectively, the

sum over thermally averaged scattering and decay rates involving the axion and their explicit expressions read

$$\bar{\Gamma}_S = \frac{g_i g_j}{32\pi^4 n_a^{\text{eq}}} T \int_{s_{\min}}^{\infty} ds \frac{\lambda(s, m_i, m_j)}{\sqrt{s}} \sigma_{ij \rightarrow ka}(s) K_1\left(\frac{\sqrt{s}}{T}\right), \quad (4.7)$$

$$\bar{\Gamma}_D = \frac{n_i^{\text{eq}}}{n_a^{\text{eq}}} \frac{K_1\left(\frac{m_i}{T}\right)}{K_2\left(\frac{m_i}{T}\right)} \gamma_{i \rightarrow ja}. \quad (4.8)$$

The function λ is defined as follows

$$\lambda(x, y, z) \equiv [x - (y + z)^2] [x - (y - z)^2], \quad (4.9)$$

whereas the minimum center of mass energy is $s_{\min} = \text{Max}((m_i + m_j)^2, m_k^2)$. The general expression for the equilibrium number density is

$$n_i^{\text{eq}} = \frac{m_i^2}{2\pi^2} T K_2\left(\frac{m_i}{T}\right) \quad (4.10)$$

where g_i stands for the degrees of freedom of the particle i and $K_n(z)$ are the modified Bessel function of the second kind.

We find it convenient to switch to dimensionless variables. We define $x = m/T$, where m is taken to be the mass of the heaviest particle in the process, and the Boltzmann equation for Y_a reads

$$sHx \frac{dY_a}{dx} = \left(1 - \frac{1}{3} \frac{\ln g_{*s}}{\ln x}\right) \sum_S \left(\gamma_S + \sum_D \gamma_D\right) \left(1 - \frac{Y_a}{Y_a^{\text{eq}}}\right), \quad (4.11)$$

where $\gamma_{D,S} \equiv n_a^{\text{eq}} \bar{\Gamma}_{D,S}$. We solve now the equation numerically for the different axion production processes. Analytical approximations can be found for the cases below thermal abundance and at large f_a , leading to $\Delta N_{\text{eff}} \propto f_a^{-8/3}$ [27].

4.1 Model Independent results

We first perform a model-independent operator analysis. For flavor conserving couplings, we switch on separately the top-axion vertex c_t and the bottom-axion vertex c_b , whereas we account for the decay of each quark for flavor violating interactions.

We begin with scatterings and we set $c_i = 1$ throughout this section; this is equivalent to interpreting f_a as f_a/c_i for each specific coupling. One of our main results is a smooth treatment of the EWPT, and this is relevant once one accounts for axion production controlled by processes with the top (anti-)quark on the external legs. We show in Fig. 1 the contribution to ΔN_{eff} from each one of these processes as a function of f_a . Production via scatterings with gluons is not altered by this threshold. However, processes with longitudinal weak gauge bosons feel this transition since they become massive below the EWPT. Dashed lines correspond to calculations in the electroweak symmetric phase whereas solid lines hold below the EWPT. Our lines for each individual process, with

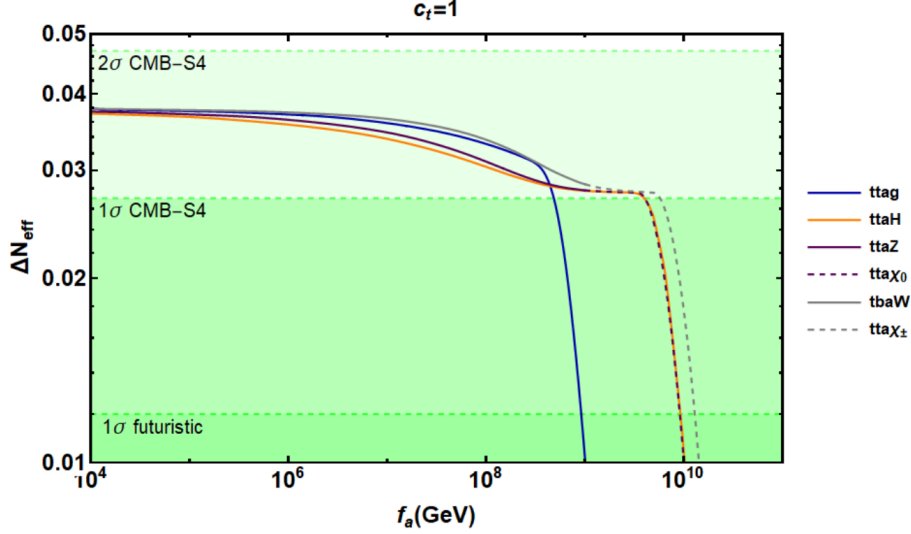


Figure 1: Contribution to ΔN_{eff} from individual binary scatterings with the top quark involved. The dimensionless coupling is set to $c_t = 1$. Each line denotes all processes with the external legs denoted in the legenda. The initial temperature here is set to $T_I = 10^4$ GeV and the initial axion abundance has been assumed to be zero.

the relevant degrees of freedom at the associated temperature, are indeed smooth across the two phases.

The physical observable is actually the combined effects of these individual lines. We add them up and we show our prediction for ΔN_{eff} in Fig. 2 together with the associated quantity from the bottom-axion vertex c_b . Solid lines correspond to the extreme case in which the initial temperature T_I (*i.e.* the reheating temperature, if the Universe went through a stage of Inflation) was very close to the EWPT, and assuming the initial abundance of axions to be zero at $T = T_I$. The opposite extreme case, dot-dashed lines, correspond to an initial thermal abundance of axions at a given initial temperature above the EWPT. Finally, we show predictions from one particular process which remains the same at all temperatures and whose strength grows with the temperature, the purely gluonic $gg \rightarrow ga$. In order to take it into account, we interpolated the result from Ref. [25] and assumed that it decreases always with the same power of temperature, extrapolating the results to lower temperatures.

Fig. 2 shows that the axion can thermalize through the scatterings with the top, below or around the EWPT, for $f_a \lesssim 10^{10}$ GeV even with zero initial axion abundance close to the EWPT. This means that, independently of the initial conditions, it is possible to be above the 1σ region of CMB-S4. If one assumes an initial thermal abundance, as shown in the same figure with dot-dashed lines, such initial seed automatically gives a signal of about 1σ , as already stressed in previous works [26].

For both choices of initial conditions, the signal increases as f_a lowers, reflecting the fact that the axion decouples at a lower temperature where the number of degrees of freedom in thermal equilibrium $g_*(T_{\text{dec}})$ is smaller. For $f_a \lesssim 10^9$ GeV the processes involving the axion-bottom coupling become efficient and yields a larger ΔN_{eff} which

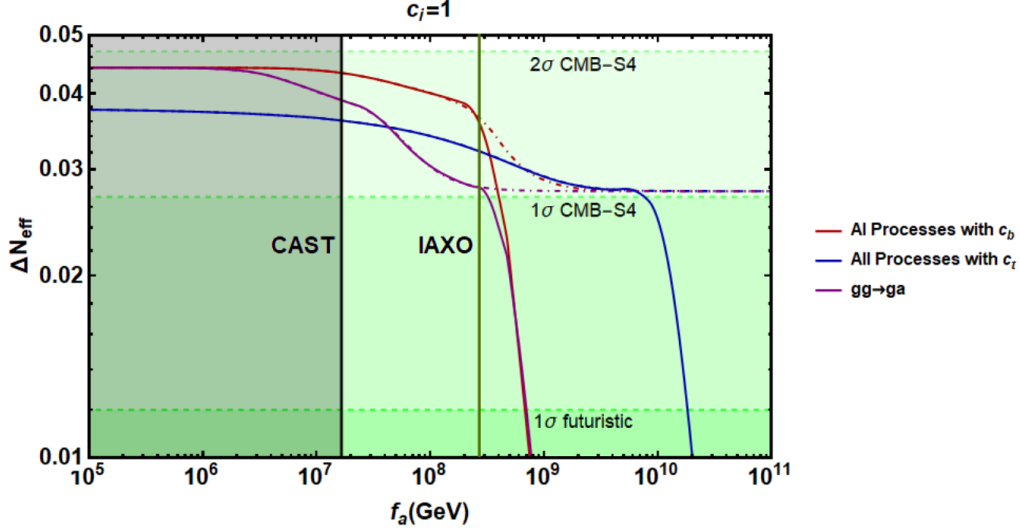


Figure 2: Impact on ΔN_{eff} following an operator-by-operator analysis: for each line, we consider the axion coupling only to one particle i , with coupling constant $c_i = 1$. The initial temperature here is set to $T_I = 10^4$ GeV and the initial axion abundance has been assumed to be zero (thermal) for the solid (dot-dashed) lines. The CAST limit and IAXO prospect are shown as a shaded region and a vertical green line respectively, assuming $c_{a\gamma\gamma} = 1$.

roughly saturates at $\Delta N_{\text{eff}}(g_*(m_b))$ for $f_a \lesssim 10^8$ GeV. Finally, we note that the axion-gluon scattering channel is always less efficient than the other scattering channels, except for $f_a \lesssim 5 \times 10^7$ GeV where it becomes more efficient than the axion-top scatterings.

We also show the constraints from CAST [38] and the forecasted sensitivity of IAXO [39, 40]. Although these experiment probe the axion-photon coupling, we can still compare both forecasts assuming $c_{a\gamma\gamma} = 1$. Interestingly, the parameter space probed by IAXO corresponds to the region where ΔN_{eff} are above the 1σ level. These multiple detection channels will be very useful in case of a detection.

As discussed in the paragraphs above, the initial conditions for our Boltzmann equation evolution depend on whether axions thermalize or not above the EWPT. For example, for $f_a \sim 10^9$ GeV the axion thermalizes already at $T \sim \text{TeV}$ due to the interactions with the Higgs [25]. In general, this depends on the value of the reheating temperature. This interplay between the axion scale f_a and the initial (reheating) temperature, when zero initial abundance is assumed for the axion, can be seen more clearly in Fig. 3. Here, we show the dependence of ΔN_{eff} on the reheating temperature and f_a by considering purely gluonic processes, which must be present in any QCD axion model, following the procedure from before. The figure shows that the axion always thermalizes, independently of f_a , as long as the reheating temperature is set high enough.

Turning now to the possibility of having flavor violating couplings, the interactions in Eq. (3.13) lead to the following possible decays below the EWPT

$$\begin{aligned} t &\rightarrow c a, & t &\rightarrow u a, \\ b &\rightarrow s a, & b &\rightarrow d a. \end{aligned} \quad (4.12)$$

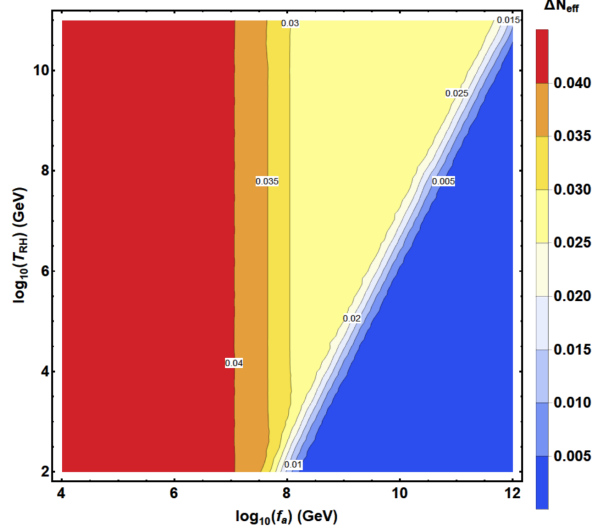


Figure 3: ΔN_{eff} as a function of f_a and the reheating temperature with initial axion abundance set to zero. In this figure only purely gluonic processes have been included.

The decays $c \rightarrow u a$ and $s \rightarrow d a$ are not taken into consideration, although they should be significant, because the relevant temperatures here should be around the QCD phase transition, where we do not have control on the complicated strongly coupled physics.

The couplings in Eq. (3.13) also lead to quark annihilation into a W and an axion with non-diagonal flavor transitions: the flavor change may be present in the coupling with the W and/or with the axion. These processes, however, are subdominant with respect to those with only flavor conserving couplings and for these reasons they are not discussed here. The only potentially interesting processes would be $t \bar{c} \rightarrow Z a$ and $t \bar{s} \rightarrow W a$, but the contribution from these processes is of the same order of magnitude as that coming from the processes that involve flavor-conserving couplings, namely $t \bar{t} \rightarrow Z a$ and $t \bar{b} \rightarrow W a$, which were already discussed above. Since the results would be essentially the same, we will not include the analysis of such processes in this work.

We show predictions for ΔN_{eff} generated from the different quark decays in Fig. 4. As already done before, we switch on only one coupling at a time. Both top decay channels yield the same ΔN_{eff} but they are subject to different bounds, and the same holds for bottom decays. In spite of the strong bounds on flavor violating couplings, given in Ref. [41] and reviewed in App. C, the signal is above 1σ in most of the cases.

Finally, we appreciate how the range of PQ breaking scales that could be detected through these hot axions in some frameworks overlap with that of cold axion dark matter. This is true for both scatterings and decays. In particular, if the PQ symmetry is broken after inflation there is an additional contribution to axion dark matter from topological defects. Axions produced non-thermally through the decays of such defects are cold, and they are a viable dark matter candidate. Although there is a large theoretical uncertainty of this contribution, we claim for the benchmark value $f_a \gtrsim \mathcal{O}(10^9)$ GeV [42, 43] it could be possible to measure both hot and cold axions at the same time.

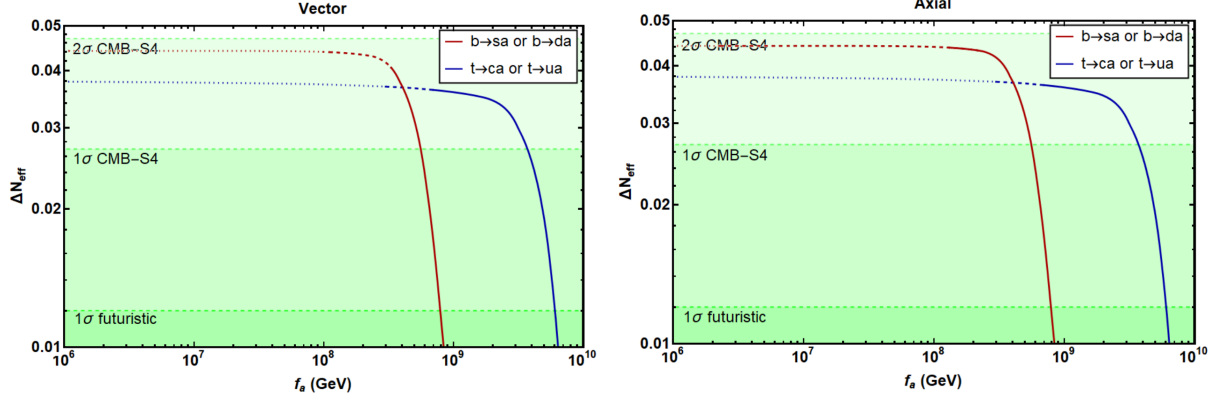


Figure 4: *Effect of quark decays on N_{eff} . The figure on the left (right) assume only vector (axial) couplings, assumed to be equal to one. In these figures solid lines escape all bounds, whereas dotted lines are ruled out. Dashed lines correspond to the situation where one of the two possible decays channels is still allowed.*

4.2 UV Complete Models

This section is devoted to the analysis of three specific models, the so-called DFSZ model [17, 18], KSVZ model [15, 16] and the Minimal Flavor Violating Axion (MFVA) model [44].

In the DFSZ case, the SM spectrum is supplemented by a second Higgs doublet and a scalar singlet. Both scalars and fermions transform under the Peccei-Quinn symmetry and, when the symmetry gets broken, an axion arises as a combination of the various Goldstone bosons. In particular, the axion couplings are flavor-blind and, using the notation of Eqs. (3.3) and (3.4), non-vanishing couplings with the top and bottom quarks are present, satisfying the following relation,

$$c_t + c_b = \frac{1}{3}. \quad (4.13)$$

In the limit where all the scalar components are heavy, except for the would-be-longitudinal components of the gauge bosons, the physical h and the axion, this model matches the general analyses performed in the previous sections. Notice that, dealing with a well-defined model, the $c_{a\gamma\gamma}$ coupling can be predicted in terms of the axion-fermion couplings: $c_{a\gamma\gamma} = 2(4c_t + c_b + 3c_\tau)$, where c_τ is the coupling with leptons and its defined in a similar way as c_t and c_b in Eqs. (3.3) and (3.4). Leptons can couple to the axion as the up-type quarks do or as the down-quarks do, and in general this leads to different values for the axion-photon coupling.

The contributions to ΔN_{eff} for the DFSZ model can be seen in Fig. 5. Three representative cases are considered, in order to cover the entire range of values for c_b and c_t : with $c_t = 1/3$ and $c_b = 0$ (in blue in the plot), with $c_t = 0$ and $c_b = 1/3$ (in red), and with $c_t = c_b = 1/6$ (in black). For the CAST limit and IAXO prospect, the continuous line corresponds to the case with the smallest value for $c_{a\gamma\gamma} = 1.92$, while the dot-dashed corresponds to the one with the most restrictive value of $c_{a\gamma\gamma} = 1.92$.

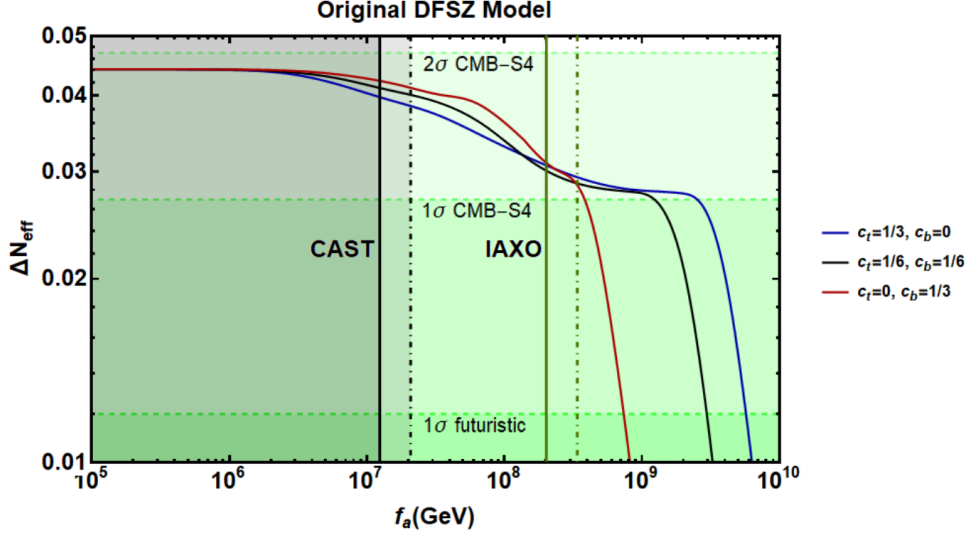


Figure 5: Total impact on ΔN_{eff} for a classic DFSZ axion. Three benchmark couplings of the DFSZ axion to top and bottom quarks have been considered. The initial temperature here is set to $T_I = 10^4 \text{ GeV}$ and the initial axion abundance has been assumed to be zero. The CAST limit and IAXO prospect are shown: solid (dot-dashed) lines correspond to $c_{a\gamma\gamma} = 8/3$ ($2/3$), when charged leptons couple to the same higgs doublet as the down-quarks (up-quarks) do.

In the KSVZ model, the axion does not couple to the SM fermions at tree-level, but only to exotic quarks that enrich the SM fermionic spectrum. In this case, only an EW singlet scalar is added to the model and the axion arises as the Goldstone boson of this field, once the Peccei-Quinn symmetry gets broken. The only sizeable contributions to ΔN_{eff} arise from the axion couplings to gluons, as axion couplings to SM fermions are induced only at 2-loops and therefore are strongly suppressed. Fig. 6 shows the predictions for ΔN_{eff} for this model. The range of axion-photon coupling considered here is $c_{a\gamma\gamma} - 1.92 \in [-0.25, 12.75]$, motivated by several possible UV completions of a KSVZ axion [45].

The MFVA model [44], instead, provides an effective description of the axion couplings with SM fields, once the flavor symmetry of the Minimal Flavor Violation framework [46, 47] is implemented in the Lagrangian. The axion couplings to fermions are universal within the same type of quarks and therefore are flavor conserving. Moreover, the axion coupling to up-type quarks is vanishing at leading order, and therefore the largest interactions are with the down-type quarks, and in particular with the bottom, due to Yukawa suppressions. This fact sensibly affects the results presented in the previous section, where the axion-top coupling was dominating all the contributions. In particular, the processes $b + \bar{b} \rightarrow g + a$ and $t + \bar{b} \rightarrow W^+ + a$ (proportional to the abb coupling), that are proportional to the bottom quark Yukawa, were irrelevant when the axion coupled to the top, but now become crucial, as they are the only important contributions apart from the purely gluonic ones.

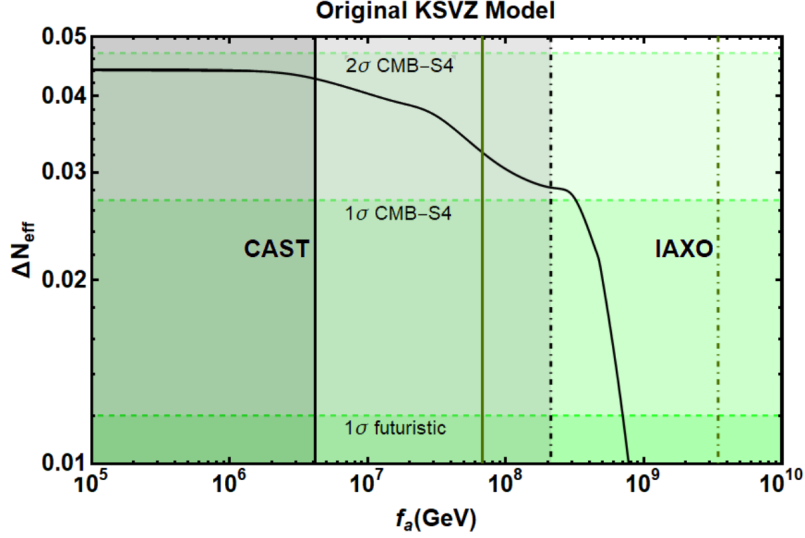


Figure 6: Total impact on ΔN_{eff} for a classic KSVZ axion. We set the initial temperature $T_I = 10^4 \text{ GeV}$ and the initial axion abundance to zero. The CAST limit is shown as a shaded region, with solid lines corresponding to $c_{a\gamma\gamma} - 1.92 = -0.25$ and dot-dashed for $c_{a\gamma\gamma} - 1.92 = 12.75$.

The coefficients describing axion couplings with bottoms c_b and with photons $g_{a\gamma\gamma}$ acquire the following values in the MFVA model,

$$c_b = \frac{1}{3}, \quad g_{a\gamma\gamma} = \frac{\alpha_{\text{em}}}{2\pi} \frac{1}{f_a} \left(\frac{8}{3} - 1.92 \right) \quad (4.14)$$

and the final result for ΔN_{eff} is shown in Fig. (7).

As it can be seen, all models give the same contribution at low f_a . At high f_a , instead, the DFSZ model gives the largest abundances since it couples to all SM fermions already at tree level. For such a model one can reach a detectable axion abundance even in the range $f_a \approx 10^9 - 10^{10} \text{ GeV}$. If the PQ symmetry is broken after inflation and not restored afterwards, the abundance of cold axion dark matter receives a significant contribution from topological defects [48–51]. The detailed amount from this source suffers a significant theoretical uncertainty [42, 43], but it is worth keeping in mind that in such a low f_a region axion cold dark matter may coexist with detectable hot axions. Within the DFSZ framework, PQ symmetry in the post inflationary scenario has to be broken also explicitly to avoid the domain wall problem [52–55].

Moreover, there is a window for f_a between 10^7 GeV and $2 \times 10^8 \text{ GeV}$ that can be explored by IAXO and is also above the 1σ level for the CMB-S4 experiments, where the models can be differentiated. This could imply an exciting opportunity to not only detect an effect of the axion, but also tell apart different invisible axion models.

When considering specific models with flavor violating axion couplings, like the Axiflavor [56] or Flaxion [57], they give a sizeable contribution to $\Delta N_{\text{eff}} \gtrsim 0.01$ only for axion scales below $f_a \lesssim 10^9 \text{ GeV}$, a region which is largely excluded in those models due to the bound coming from the $K^+ \rightarrow \pi^+ a$ decay, being therefore irrelevant in this analysis.

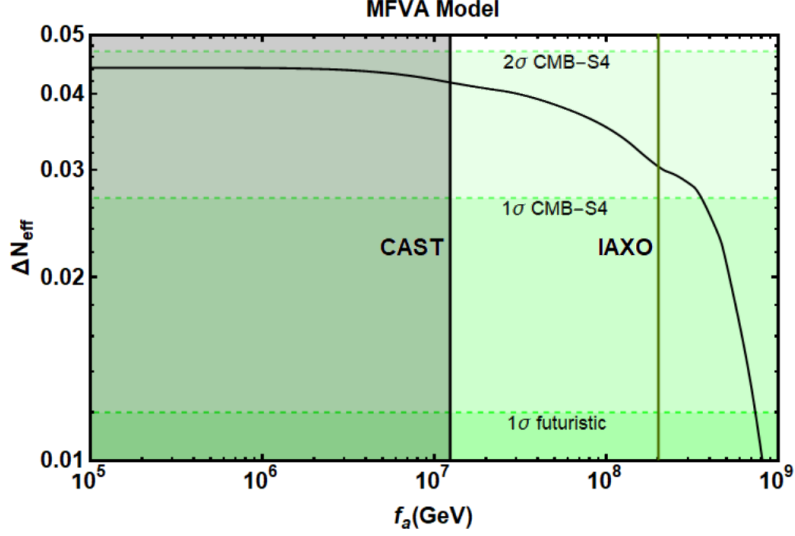


Figure 7: Total impact on ΔN_{eff} for the MFVA model. The initial temperature here is set to $T_I = 10^4$ GeV and the initial axion abundance is set to zero. The CAST limit and IAXO prospect are shown as a shaded region and a vertical green line, respectively.

5 Conclusions

The QCD axion is one of the best motivated candidates for physics beyond the SM. It provides an elegant dynamical solution to the strong CP problem and it is also a viable DM candidate. Recently, the community put forward a wealth of new ideas and techniques to detect such an elusive degree of freedom [14]. These experiments look for either virtual effects of a light pseudo-scalar mediator generating a new long range force or the axion DM wind within our Milky Way.

There is an axion complementary probe within the reach of future experiments. Hot axions can be produced from scatterings or decays of thermal bath particles in the early universe, and they remain relativistic subsequently until the time of matter/radiation equality and recombination; this is true as long as $m_a \ll \mathcal{O}(0.1)$ eV, as we consider in this work by neglecting the axion mass. They would manifest themselves in the CMB anisotropy spectrum as an additional radiation component, parameterized as the number of additional effective neutrinos ΔN_{eff} .

In this work, we studied axions couplings to third generation quarks and we provided rigorous predictions for ΔN_{eff} . We considered flavor conserving couplings, in which case production is controlled by binary collisions, and we also considered flavor violating couplings leading to axion production via two-body decays. We computed scattering cross sections and decay widths, and we obtained predictions for ΔN_{eff} after solving numerically the Boltzmann equation tracking the axion number density. Our predictions are smooth across the EWPT.

Our results can be found in Sec. 4. We studied both the model-independent contribution based on switching on an effective operator at a time as well as specific UV complete models. We found parameter space regions for all cases, typically with PQ

breaking scale in the range $f_a \sim (10^9 - 10^{10})$ GeV for order one couplings to fermions, where the predicted signal is comparable to the forecasted 1σ sensitivity of CMB S4 experiments, and it could be detectable by more futuristic experiments.

Finally, we point out two complementary signals. The values of the PQ breaking scale leading to an observable effect on ΔN_{eff} is consistent with axion cold dark matter. Furthermore, if there is no substantial hierarchy between the dimensionless axion couplings considered in this work and the associated one to photons then future helioscopes are also able to probe this parameter space region. The complementarity of these possible signals makes for a quite fascinating probe into the nature of the axion itself.

Acknowledgments. F.A.A and L.M. acknowledge partial financial support by the Spanish MINECO through the Centro de excelencia Severo Ochoa Program under grant SEV-2016-0597, by the Spanish “Agencia Estatal de Investigación”(AEI) and the EU “Fondo Europeo de Desarrollo Regional” (FEDER) through the projects FPA2016-78645-P and PID2019-108892RB-I00/AEI/10.13039/501100011033. F.A.A, F.D. and L.M. acknowledge support from the European Union’s Horizon 2020 research and innovation programme under the Marie Skłodowska-Curie grant agreement No 860881-HIDDeN. The work of F.D. is supported by the grants: “New Theoretical Tools for Axion Cosmology” under the Supporting Talent in ReSearch@University of Padova (STARS@UNIPD), “The Dark Universe: A Synergic Multi- messenger Approach” number 2017X7X85K under the program PRIN 2017 funded by the Ministero dell’Istruzione, Università e della Ricerca (MIUR), “New Theoretical Tools to Look at the Invisible Universe” funded by the University of Padua. F.D. is also supported and by Istituto Nazionale di Fisica Nucleare (INFN) through the Theoretical Astroparticle Physics (TAsP) project. L.M. acknowledges partial financial support by the Spanish MINECO through the “Ramón y Cajal” programme (RYC-2015-17173). RZF acknowledges support by the Spanish Ministry MEC under grant FPA 2017-88915-P and the Severo Ochoa excellence program of MINECO (SEV-2016- 0588).

A Operator basis for axion couplings to quarks

In this appendix, we define the field basis for SM quarks that we employ in our analysis. The part of the SM Lagrangian needed for this discussion is the one containing Yukawa interactions. Focusing on quarks, the most generic set of Yukawa terms reads

$$- \mathcal{L}_Y = \overline{Q_L''} \tilde{H} Y^u u_R'' + \overline{Q_L''} H Y^d d_R'' + \text{h.c.} . \quad (\text{A.1})$$

The fields appearing in the operators above are: $SU(2)_L$ quark doublets Q_L'' , $SU(2)_L$ quark singlets u_R'' and d_R'' and the $SU(2)_L$ Higgs doublet field H . Moreover, we define $\tilde{H} \equiv i\sigma_2(H^\dagger)^T$ and $Y^{u,d}$ are generic 3×3 diagonalizable matrices in flavor space. We save the symbol of unprimed fields for quark mass eigenstates defined later.

We diagonalize the Yukawa matrices by performing bi-unitary transformations

$$Y^u = U_{u_L} \hat{Y}^u U_{u_R}^\dagger, \quad Y^d = U_{d_L} \hat{Y}^d U_{d_R}^\dagger, \quad (\text{A.2})$$

where the U matrices are unitary and the hatted quantities are diagonal in flavor space. We introduce a new set of prime fields defined as follows

$$Q_L'' = U_{u_L} Q_L', \quad u_R'' = U_{u_R} u_R', \quad d_R'' = U_{d_R} d_R', \quad (\text{A.3})$$

The Yukawa Lagrangian in the new basis reads

$$- \mathcal{L}_Y = \overline{Q_L'} \tilde{H} \hat{Y}^u u_R' + \overline{Q_L'} H V_{\text{CKM}} \hat{Y}^d d_R' + \text{h.c.}, \quad (\text{A.4})$$

with $V_{\text{CKM}} \equiv U_{u_L}^\dagger U_{d_L}$ the CKM matrix. In our study, we always specify axion couplings in the primed field basis for quarks with Yukawa interactions as in Eq. (A.4).

Finally, we identify the quark mass eigenstates, which we denote with unprimed fields, and their relation to the primed fields. First, we identify the components of the quark doublet $Q_L' = (u_L' \ d_L')$. Once the Higgs gets a vacuum expectation value (vev), we identify mass eigenstates by redefining the left-handed down quarks

$$u_L' = u_L, \quad d_L' = V_{CKM} d_L, \quad u_R' = u_R, \quad d_R' = d_R, \quad (\text{A.5})$$

Flavor eigenstates u_i' coincide with the mass eigenstates u_i , and the b' quark, the only down-quark we are interested in, almost coincides with the b quark up to CKM corrections of order $\mathcal{O}(0.05)$. In contrast to gauge interactions in the primed basis, which are still flavor diagonal, the CKM matrix appears in the fermion charged current once we switch to mass eigenstates

$$J_\mu^- = \overline{u_L} \gamma_\mu V_{\text{CKM}} d_L. \quad (\text{A.6})$$

B Cross sections below the EWPT

We provide analytical cross sections for the processes listed in Tab. 2, and we begin with the first block where the two particles in the initial state are fermions. A quark can find its own antiparticle and annihilate to final states containing one axion particle. If the final state is the gluon we have quark-antiquark annihilations to gluon and axion with a cross section

$$\sigma_{q\bar{q} \rightarrow ga} = \frac{c_q^2 g_s^2 m_q^2}{9\pi f_a^2 (s - 4m_q^2)} \tanh^{-1} \sqrt{1 - \frac{4m_q^2}{s}} \left(\right), \quad (\text{B.1})$$

where g_s is the strong coupling constant and s is the usual Mandelstam variable denoting the (squared of the) energy in the center of mass frame. Here and below, we denote with the letter $q = \{t, b\}$ a generic third generation quark when it is possible to provide a single expression valid for both cases. If the other SM particle in the final state is the Higgs boson we have

$$\sigma_{q\bar{q} \rightarrow ha}^\downarrow = \frac{c_q^2 y_q^2 (s - m_h^2)}{64\pi s f_a^2 (s - 4m_q^2)} \sqrt{s(s - 4m_q^2) - 4m_q^2} \tanh^{-1} \sqrt{\left(\frac{4m_q^2}{s} \right)} \left(\right) \quad (\text{B.2})$$

where the symbol “ \downarrow ” indicates that cross sections are calculated below the EWPT. Likewise, quarks can annihilate with their own antiquarks leading to an axion final state together with the Z boson with cross sections

$$\sigma_{t\bar{t} \rightarrow Za} = \frac{c_t^2 g_W^2 m_t^2 \sqrt{\frac{1}{s-4m_t^2}} (s-m_Z^2)}{1152\pi s^{3/2} f_a^2 m_W^2 m_Z^2} 4 \sqrt{\left(\frac{s}{s-4m_t^2} \tanh^{-1} \sqrt{1-\frac{4m_t^2}{s}}\right)} \left(-m_Z^2 (9m_t^2 + 40m_W^2) + 32m_W^4 + 17m_Z^4\right) + 9m_Z^2 (s-2m_Z^2) \Big) \Big) \quad (\text{B.3})$$

$$\sigma_{b\bar{b} \rightarrow Za} = \frac{c_b^2 g_W^2 m_b^2 \sqrt{\frac{1}{s-4m_b^2}} (s-m_Z^2)}{1152\pi s^{3/2} f_a^2 m_W^2 m_Z^2} 4 \sqrt{\left(\frac{s}{s-4m_b^2} \tanh^{-1} \sqrt{1-\frac{4m_b^2}{s}}\right)} \left(-m_Z^2 (9m_b^2 + 4m_W^2) + 8m_W^4 + 5m_Z^4\right) + 9m_Z^2 (s-2m_Z^2) \Big) \Big), \quad (\text{B.4})$$

Finally, to complete the first block of the table, we can have a top quark and a bottom antiquark as well as the CP conjugate system annihilating to a final state with an axion and a W boson with cross section

$$\begin{aligned} \sigma_{t\bar{b} \rightarrow W+a} = & \frac{g_W^2 (s-m_W^2)}{128\pi s f_a^2 m_W^2 \left((-m_b^2+m_t^2+s)^2 - 4sm_t^2\right)} \left((c_b^2 m_b^2 + c_t^2 m_t^2) (s-2m_W^2) \sqrt{-2m_b^2(m_t^2+s) + m_b^4 + (m_t^2-s)^2} + \right. \\ & - 2c_t^2 m_t^2 s (m_b^2 - m_t^2 + 2m_W^2) \coth^{-1} \frac{m_b^2 - m_t^2 - s}{\sqrt{-2m_b^2(m_t^2+s) + m_b^4 + (m_t^2-s)^2}} \Big) \Big(\\ & + 2c_b m_b^2 s \left(2 \left(c_t m_t^2 \coth^{-1} \frac{m_b^2 + m_t^2 - s}{\sqrt{-2m_b^2(m_t^2+s) + m_b^4 + (m_t^2-s)^2}} \right) \Big(\right. \\ & \left. \left. + c_b (m_t^2 - m_b^2 + 2m_W^2) \coth^{-1} \frac{m_b^2 - m_t^2 + s}{\sqrt{-2m_b^2(m_t^2+s) + m_b^4 + (m_t^2-s)^2}} \right) \right) \Big) \Big) \quad (\text{B.5}) \end{aligned}$$

We switch to the second block of Tab. 2 and we consider when there is just one fermion in the initial and final states. For a gluon in the initial state we find

$$\sigma_{qg \rightarrow qa} = \frac{c_q^2 g_s^2 m_q^2}{192\pi f_a^2 s^2 (s-m_q^2)} \left[2s^2 \log \left(\frac{s}{m_q^2} \right) \left(4sm_q^2 - m_q^4 - 3s^2 \right) \right]. \quad (\text{B.6})$$

For quark/Higgs boson scattering we have

$$\begin{aligned} \sigma_{qh \rightarrow qa}^\downarrow = & \frac{c_q^2 g_q^2 (s-m_q^2)}{64\pi s f_a^2 \left((-m_h^2+m_q^2+s)^2 - 4sm_q^2\right)} \left[\left((-m_h^2+m_q^2+s) \sqrt{-2m_h^2(m_q^2+s) + m_h^4 + (m_q^2-s)^2} + \right. \right. \\ & \left. \left. - 2sm_q^2 \log \left(\frac{\sqrt{-2m_h^2(m_q^2+s) + m_h^4 + (m_q^2-s)^2} - m_h^2 + m_q^2 + s}{\sqrt{-2m_h^2(m_q^2+s) + m_h^4 + (m_q^2-s)^2} + m_h^2 - m_q^2 - s} \right) \right) \right] \quad (\text{B.7}) \end{aligned}$$

whereas for the case of a Z boson we find

$$\begin{aligned} \sigma_{tZ \rightarrow ta} = & \frac{c_t^2 g_W^2 m_t^2 (s-m_t^2)}{3456\pi s^2 f_a^2 m_W^2 m_Z^2 \sqrt{(m_t^2 - m_Z^2 + s)^2 - 4sm_t^2}} \times \\ & 2s^2 (m_Z^2 (9m_t^2 + 40m_W^2) - 32m_W^4 - 17m_Z^4) \log \left(\frac{-\sqrt{-2m_t^2(m_Z^2+s) + m_t^4 + (m_Z^2-s)^2} + m_t^2 - m_Z^2 + s}{\sqrt{-2m_t^2(m_Z^2+s) + m_t^4 + (m_Z^2-s)^2} + m_t^2 - m_Z^2 + s} \right) \\ & \times \frac{\sqrt{-2m_t^2(m_Z^2+s) + m_t^4 + (m_Z^2-s)^2}}{\sqrt{-2m_t^2(m_Z^2+s) + m_t^4 + (m_Z^2-s)^2}} + \\ & + 3s (m_Z^2 (3m_t^2 + 40m_W^2) - 32m_W^4 - 8m_Z^4) + (m_t - m_Z)(m_t + m_Z) (-40m_W^2 m_Z^2 + 32m_W^4 + 17m_Z^4) + 9s^2 m_Z^2 \Big) \Big) \quad (\text{B.8}) \end{aligned}$$

$$\begin{aligned}
\sigma_{bZ \rightarrow ba} = & \frac{c_b^2 g_W^2 m_b^2 (s - m_b^2)}{3456 \pi s^2 f_a^2 m_W^2 m_Z^2 \sqrt{(m_b^2 - m_Z^2 + s)^2 - 4 s m_b^2}} \times \\
& \times \frac{2s^2 (m_Z^2 (9m_b^2 + 4m_W^2) - 8m_W^4 - 5m_Z^4) \log \left(\frac{-\sqrt{-2m_b^2 (m_Z^2 + s) + m_b^4 + (m_Z^2 - s)^2} + m_b^2 - m_Z^2 + s}{\sqrt{-2m_b^2 (m_Z^2 + s) + m_b^4 + (m_Z^2 - s)^2} + m_b^2 - m_Z^2 + s} \right)}{\sqrt{-2m_b^2 (m_Z^2 + s) + m_b^4 + (m_Z^2 - s)^2}} + \\
& + 3s (m_Z^2 (3m_b^2 + 4m_W^2) - 8m_W^4 + 4m_Z^4) + (m_b - m_Z)(m_b + m_Z) (-4m_W^2 m_Z^2 + 8m_W^4 + 5m_Z^4) + 9s^2 m_Z^2 \Bigg) \Bigg(\quad (B.9)
\end{aligned}$$

Finally, if the initial state quark annihilate with a W boson we have the cross sections

$$\begin{aligned}
\sigma_{tW^- \rightarrow ba} = & \frac{g_W^2 (s - m_b^2)}{384 \pi s^2 f_a^2 m_W^2 ((m_t^2 - m_W^2 + s)^2 - 4 s m_t^2)} \sqrt{-2m_t^2 (m_W^2 + s) + (m_W^2 - s)^2 + m_t^4} \Bigg(2c_b c_t m_b^2 m_t^2 (3s + m_W^2 - m_t^2) + \\
& + c_b^2 m_b^2 (m_t^4 - 2m_W^4 + m_t^2 (m_W^2 - 2s) + m_W^2 s + s^2) + c_t^2 m_t^2 (m_b^2 (m_t^2 - m_W^2 - 3s) + s (m_t^2 - m_W^2 + s)) \Bigg) \Bigg(\\
& + 2s^2 c_t m_t^2 (2c_b m_b^2 + c_t (m_t^2 - m_b^2 - 2m_W^2)) \log \left(\frac{(m_t^2 - m_W^2 + s - \sqrt{-2m_t^2 (m_W^2 + s) + (m_W^2 - s)^2 + m_t^4})}{(m_t^2 - m_W^2 + s + \sqrt{-2m_t^2 (m_W^2 + s) + (m_W^2 - s)^2 + m_t^4})} \right) \Bigg) \Bigg), \quad (B.10)
\end{aligned}$$

$$\begin{aligned}
\sigma_{bW^+ \rightarrow ta} = & \frac{g_W^2 (s - m_t^2)}{384 \pi s^2 f_a^2 m_W^2 ((m_b^2 - m_W^2 + s)^2 - 4 s m_b^2)} \sqrt{-2m_b^2 (m_W^2 + s) + (m_W^2 - s)^2 + m_b^4} \Bigg(2c_t c_b m_t^2 m_b^2 (3s + m_W^2 - m_b^2) + \\
& + c_t^2 m_t^2 (m_b^4 - 2m_W^4 + m_b^2 (m_W^2 - 2s) + m_W^2 s + s^2) + c_b^2 m_b^2 (m_t^2 (m_b^2 - m_W^2 - 3s) + s (m_b^2 - m_W^2 + s)) \Bigg) \Bigg(\\
& + 2s^2 c_b m_b^2 (2c_t m_t^2 + c_b (m_b^2 - m_t^2 - 2m_W^2)) \log \left(\frac{(m_b^2 - m_W^2 + s - \sqrt{-2m_b^2 (m_W^2 + s) + (m_W^2 - s)^2 + m_b^4})}{(m_b^2 - m_W^2 + s + \sqrt{-2m_b^2 (m_W^2 + s) + (m_W^2 - s)^2 + m_b^4})} \right) \Bigg) \Bigg), \quad (B.11)
\end{aligned}$$

C Bounds on axion couplings

In this Appendix, we collect astrophysical, cosmological and terrestrial experimental bounds on axion interactions with SM particles given in Sec. 2.

Coupling with photons. The effective coupling to photons, as defined in Eq. (2.4), must satisfy the following constraints [10, 11, 13, 58]:

$$\begin{aligned}
|g_{a\gamma\gamma}| & \lesssim 7 \times 10^{-11} \text{ GeV}^{-1} & \text{for } m_a & \lesssim 10 \text{ meV} \\
|g_{a\gamma\gamma}| & \lesssim 10^{-10} \text{ GeV}^{-1} & \text{for } 10 \text{ meV} & \lesssim m_a \lesssim 1 \text{ eV} \\
|g_{a\gamma\gamma}| & \ll 10^{-12} \text{ GeV}^{-1} & \text{for } 10 \text{ eV} & \lesssim m_a \lesssim 0.1 \text{ GeV} \\
|g_{a\gamma\gamma}| & \lesssim 10^{-3} \text{ GeV}^{-1} & \text{for } 0.1 \text{ GeV} & \lesssim m_a \lesssim 1 \text{ TeV}.
\end{aligned} \quad (C.1)$$

For masses larger than the TeV, no constraint is present on these couplings. These bounds can be translated in terms of f_a once a specific value of $c_{a\gamma\gamma}$ is taken.

Axion flavor conserving couplings to third generation quarks. Stellar cooling data imply bounds on axion couplings to top and bottom quarks [59]. In general, this constraint applies on the effective axion coupling with electrons, which is the sum between the tree-level coupling with electrons and the loop-induced contributions proportional to the axion couplings with any other fermion. Under the assumption that only one coupling is non-vanishing at a time, and in particular the tree level coupling with electrons is zero, then

$$\frac{f_a}{c_t} \gtrsim 1.2 \times 10^9 \text{ GeV} \quad \frac{f_a}{c_b} \gtrsim 6.1 \times 10^5 \text{ GeV}, \quad (\text{C.2})$$

for axion masses in the range $m_a \lesssim 10 \text{ keV}$.

Axion couplings to nucleons. Neutron star and Supernova SN1987A cooling data provide bounds on axion coupling with neutrons and nuclei. The physical process consists in the neutron or nucleus bremsstrahlung, respectively, and the corresponding bounds read

$$\frac{f_a}{c_{an}} > 1.21 \times 10^9 \text{ GeV} [60, 61] \quad \frac{f_a}{\sqrt{c_{ap}^2 + c_{an}^2}} > 1.67 \times 10^9 \text{ GeV} [62, 63], \quad (\text{C.3})$$

where c_{an} and c_{ap} stand for the effective coupling of axion to neutrons and protons and are expressed in terms of the axion-quark couplings as follows:

$$\begin{aligned} c_{an} &= -0.02 + 0.88c_d - 0.39c_u - 0.038c_s - 0.012c_c - 0.009c_b - 0.0035c_t, \\ c_{ap} &= -0.47 + 0.88c_u - 0.39c_d - 0.038c_s - 0.012c_c - 0.009c_b - 0.0035c_t. \end{aligned} \quad (\text{C.4})$$

The constant terms refer to the axion coupling to gluons, while the others to the corresponding axion-fermion couplings. These bounds are rather strong, but should be taken with caution: from one side they are model dependent and from the other hold under the current knowledge of the complicated Supernova physics and neutron stars. If one considers only the couplings c_t and c_b , as we do in our work, these bounds are sub-dominant with respect to the ones in Eq. (C.2).

Axion flavor violating couplings to third generation quarks. Flavor violating coupling are strongly constrained from processes like rare decays or meson oscillations. An example of these processes are $B^+ \rightarrow \pi^+ a$ decay and $B^0 - \bar{B}^0$ oscillations, from where a bound can be obtained on the vector and axial axion coupling, respectively, to bottom and down quarks [41, 64, 65]:

$$\frac{f_a}{c_{bd}^V} > 1.1 \times 10^8 \text{ GeV} \quad \frac{f_a}{c_{bd}^A} > 2.6 \times 10^6 \text{ GeV}. \quad (\text{C.5})$$

Analogously, from the processes $B^{+,0} \rightarrow K^{+,0} a$ and $B^{+,0} \rightarrow K^{*+,0} a$ bounds on the vector and axial couplings to bottom and strange quarks can be obtained [66]:

$$\frac{f_a}{c_{bs}^V} > 3.3 \times 10^8 \text{ GeV} \quad \frac{f_a}{c_{bs}^A} > 1.3 \times 10^8 \text{ GeV}. \quad (\text{C.6})$$

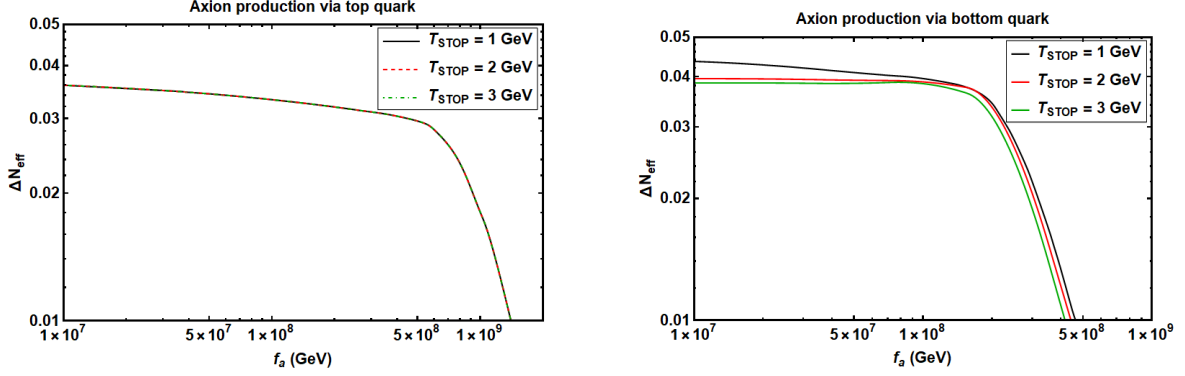


Figure 8: Sensitivity of the ΔN_{eff} prediction on the lowest temperature T_{STOP} reached by our Boltzmann equation integration. We choose values of T_{STOP} close to the QCDPT, and we show results for production via top (left panel) and bottom (right panel) scattering.

Bounds of flavor violating couplings involving the top quark are obtained in the same fashion as for the flavor conserving ones: considering the contribution at one loop to the process $K^+ \rightarrow \pi^+ a$ of a top-up and top-charm coupling it is possible to extract the following bounds [67]:

$$\frac{f_a}{c_{tu}} > 3 \times 10^8 \text{ GeV} \quad \frac{f_a}{c_{tc}} > 7 \times 10^8 \text{ GeV}. \quad (\text{C.7})$$

D Approaching the QCDPT

Ideally, we should integrate the Boltzmann equation tracking the axion number density all the way down to very low temperatures in order to predict ΔN_{eff} . We have seen why this is not necessary because the axion comoving density reaches an asymptotic value once SM quarks participating in the production starts feeling the Maxwell-Boltzmann suppression. So it is enough to stop our Boltzmann equation integration at some IR temperature cutoff that we denote T_{STOP} .

The value of the needed T_{STOP} could be dangerous if it is too low. Our analysis is based on perturbative calculations for scattering cross sections and on treating the primordial bath as a gas of weakly-coupled quarks and gluons in thermal equilibrium. This setup is certainly valid at high temperatures around the EWPT, and it loses its validity as we approach the QCDPT. In this appendix, we investigate how robust is our predictions for ΔN_{eff} considering this potential issue.

We show in Fig. 8 the prediction for ΔN_{eff} as a function of f_a for axion production via top quark (left panel) and bottom quark (right panel) scatterings. In each panel, we report our prediction for the different values $T_{\text{STOP}} = \{1, 2, 3\}$ GeV close to the QCDPT. The result for the top is absolutely stable, and this is not surprising since the top mass is much larger than the typical temperatures around the QCDPT. On the contrary, production via bottom scattering presents some dependence on this temperature and decreasing it leads to slightly higher ΔN_{eff} . However, such a dependence on T_{STOP} is noticeable mostly in the region of very low PQ breaking scales ruled out by experiments. Thus,

our results are robust. And, in any case, they could be interpreted as a lower bound on the expected effect on ΔN_{eff} that still ensures perturbativity in the computations.

References

- [1] C.A. Baker et al., *An Improved Experimental Limit on the Electric Dipole Moment of the Neutron*, *Phys. Rev. Lett.* **97** (2006) 131801 [[hep-ex/0602020](#)].
- [2] J.M. Pendlebury et al., *Revised Experimental Upper Limit on the Electric Dipole Moment of the Neutron*, *Phys. Rev.* **D92** (2015) 092003 [[1509.04411](#)].
- [3] R.D. Peccei and H.R. Quinn, *CP Conservation in the Presence of Instantons*, *Phys. Rev. Lett.* **38** (1977) 1440.
- [4] R.D. Peccei and H.R. Quinn, *Constraints Imposed by CP Conservation in the Presence of Instantons*, *Phys. Rev.* **D16** (1977) 1791.
- [5] F. Wilczek, *Problem of Strong P and T Invariance in the Presence of Instantons*, *Phys. Rev. Lett.* **40** (1978) 279.
- [6] S. Weinberg, *A New Light Boson?*, *Phys. Rev. Lett.* **40** (1978) 223.
- [7] C. Vafa and E. Witten, *Parity Conservation in QCD*, *Phys. Rev. Lett.* **53** (1984) 535.
- [8] W.A. Bardeen, S.H.H. Tye and J.A.M. Vermaseren, *Phenomenology of the New Light Higgs Boson Search*, *Phys. Lett.* **76B** (1978) 580.
- [9] G. Grilli di Cortona, E. Hardy, J. Pardo Vega and G. Villadoro, *The QCD Axion, Precisely*, *JHEP* **01** (2016) 034 [[1511.02867](#)].
- [10] CAST collaboration, *New Cast Limit on the Axion-Photon Interaction*, *Nature Phys.* **13** (2017) 584 [[1705.02290](#)].
- [11] J. Jaeckel and M. Spannowsky, *Probing MeV to 90 GeV Axion-Like Particles with Lep and Lhc*, *Phys. Lett.* **B753** (2016) 482 [[1509.00476](#)].
- [12] I. Brivio, M.B. Gavela, L. Merlo, K. Mimasu, J.M. No, R. del Rey et al., *Alps Effective Field Theory and Collider Signatures*, *Eur. Phys. J.* **C77** (2017) 572 [[1701.05379](#)].
- [13] M. Bauer, M. Neubert and A. Thamm, *Collider Probes of Axion-Like Particles*, *JHEP* **12** (2017) 044 [[1708.00443](#)].
- [14] I.G. Irastorza and J. Redondo, *New experimental approaches in the search for axion-like particles*, *Prog. Part. Nucl. Phys.* **102** (2018) 89 [[1801.08127](#)].
- [15] J.E. Kim, *Weak Interaction Singlet and Strong CP Invariance*, *Phys. Rev. Lett.* **43** (1979) 103.

- [16] M.A. Shifman, A.I. Vainshtein and V.I. Zakharov, *Can Confinement Ensure Natural CP Invariance of Strong Interactions?*, *Nucl. Phys.* **B166** (1980) 493.
- [17] A.R. Zhitnitsky, *On Possible Suppression of the Axion Hadron Interactions*. (In Russian), *Sov. J. Nucl. Phys.* **31** (1980) 260.
- [18] M. Dine, W. Fischler and M. Srednicki, *A Simple Solution to the Strong CP Problem with a Harmless Axion*, *Phys. Lett.* **B104** (1981) 199.
- [19] D.J.E. Marsh, *Axion Cosmology*, *Phys. Rept.* **643** (2016) 1 [[1510.07633](#)].
- [20] M.S. Turner, *Thermal Production of Not SO Invisible Axions in the Early Universe*, *Phys. Rev. Lett.* **59** (1987) 2489.
- [21] E. Masso, F. Rota and G. Zsembinszki, *On axion thermalization in the early universe*, *Phys. Rev.* **D66** (2002) 023004 [[hep-ph/0203221](#)].
- [22] CMB-S4 collaboration, *CMB-S4 Science Book, First Edition*, [1610.02743](#).
- [23] K. Abazajian et al., *CMB-S4 Science Case, Reference Design, and Project Plan*, [1907.04473](#).
- [24] C. Brust, D.E. Kaplan and M.T. Walters, *New Light Species and the CMB*, *JHEP* **12** (2013) 058 [[1303.5379](#)].
- [25] A. Salvio, A. Strumia and W. Xue, *Thermal axion production*, *JCAP* **1401** (2014) 011 [[1310.6982](#)].
- [26] D. Baumann, D. Green and B. Wallisch, *New Target for Cosmic Axion Searches*, *Phys. Rev. Lett.* **117** (2016) 171301 [[1604.08614](#)].
- [27] R.Z. Ferreira and A. Notari, *Observable Windows for the QCD Axion Through the Number of Relativistic Species*, *Phys. Rev. Lett.* **120** (2018) 191301 [[1801.06090](#)].
- [28] F. D'Eramo, R.Z. Ferreira, A. Notari and J.L. Bernal, *Hot Axions and the H_0 tension*, *JCAP* **1811** (2018) 014 [[1808.07430](#)].
- [29] XENON collaboration, *Excess electronic recoil events in XENON1T*, *Phys. Rev. D* **102** (2020) 072004 [[2006.09721](#)].
- [30] F. Arias-Aragon, F. D'Eramo, R.Z. Ferreira, L. Merlo and A. Notari, *Cosmic Imprints of XENON1T Axions*, *JCAP* **11** (2020) 025 [[2007.06579](#)].
- [31] J.L. Bernal, L. Verde and A.G. Riess, *The trouble with H_0* , *JCAP* **1610** (2016) 019 [[1607.05617](#)].
- [32] H. Georgi, D.B. Kaplan and L. Randall, *Manifesting the Invisible Axion at Low-Energies*, *Phys. Lett.* **B169** (1986) 73.
- [33] D.B. Kaplan, *Opening the Axion Window*, *Nucl. Phys.* **B260** (1985) 215.

- [34] M. Srednicki, *Axion Couplings to Matter. 1. CP Conserving Parts*, *Nucl. Phys.* **B260** (1985) 689.
- [35] W.A. Bardeen, R.D. Peccei and T. Yanagida, *Constraints on Variant Axion Models*, *Nucl. Phys.* **B279** (1987) 401.
- [36] B.D. Fields, K.A. Olive, T.-H. Yeh and C. Young, *Big-Bang Nucleosynthesis After Planck*, *JCAP* **03** (2020) 010 [[1912.01132](#)].
- [37] PLANCK collaboration, *Planck 2018 results. VI. Cosmological parameters*, [1807.06209](#).
- [38] CAST collaboration, *Probing eV-scale axions with CAST*, *JCAP* **0902** (2009) 008 [[0810.4482](#)].
- [39] I.G. Irastorza et al., *Towards a New Generation Axion Helioscope*, *JCAP* **1106** (2011) 013 [[1103.5334](#)].
- [40] E. Armengaud et al., *Conceptual Design of the International Axion Observatory (IAXO)*, *JINST* **9** (2014) T05002 [[1401.3233](#)].
- [41] J. Martin Camalich, M. Pospelov, P.N.H. Vuong, R. Ziegler and J. Zupan, *Quark Flavor Phenomenology of the QCD Axion*, *Phys. Rev. D* **102** (2020) 015023 [[2002.04623](#)].
- [42] M. Gorghetto, E. Hardy and G. Villadoro, *Axions from Strings: the Attractive Solution*, *JHEP* **07** (2018) 151 [[1806.04677](#)].
- [43] M. Gorghetto, E. Hardy and G. Villadoro, *More Axions from Strings*, [2007.04990](#).
- [44] F. Arias-Aragon and L. Merlo, *The Minimal Flavour Violating Axion*, *JHEP* **10** (2017) 168 [[1709.07039](#)].
- [45] L. Di Luzio, F. Mescia and E. Nardi, *The Window for Preferred Axion Models*, [1705.05370](#).
- [46] R. Chivukula and H. Georgi, *Composite Technicolor Standard Model*, *Phys. Lett. B* **188** (1987) 99.
- [47] G. D'Ambrosio, G. Giudice, G. Isidori and A. Strumia, *Minimal flavor violation: An Effective field theory approach*, *Nucl. Phys. B* **645** (2002) 155 [[hep-ph/0207036](#)].
- [48] A. Vilenkin and A. Everett, *Cosmic Strings and Domain Walls in Models with Goldstone and PseudoGoldstone Bosons*, *Phys. Rev. Lett.* **48** (1982) 1867.
- [49] T. Vachaspati, A.E. Everett and A. Vilenkin, *Radiation From Vacuum Strings and Domain Walls*, *Phys. Rev. D* **30** (1984) 2046.
- [50] S. Chang, C. Hagmann and P. Sikivie, *Studies of the motion and decay of axion walls bounded by strings*, *Phys. Rev. D* **59** (1999) 023505 [[hep-ph/9807374](#)].

- [51] C. Hagmann, S. Chang and P. Sikivie, *Axion radiation from strings*, *Phys. Rev. D* **63** (2001) 125018 [[hep-ph/0012361](#)].
- [52] A. Vilenkin, *Gravitational Field of Vacuum Domain Walls and Strings*, *Phys. Rev. D* **23** (1981) 852.
- [53] P. Sikivie, *Of Axions, Domain Walls and the Early Universe*, *Phys. Rev. Lett.* **48** (1982) 1156.
- [54] J. Ipser and P. Sikivie, *The Gravitationally Repulsive Domain Wall*, *Phys. Rev. D* **30** (1984) 712.
- [55] A. Vilenkin, *Gravitational Field of Vacuum Domain Walls*, *Phys. Lett. B* **133** (1983) 177.
- [56] L. Calibbi, F. Goertz, D. Redigolo, R. Ziegler and J. Zupan, *Minimal axion model from flavor*, *Phys. Rev. D* **95** (2017) 095009 [[1612.08040](#)].
- [57] Y. Ema, K. Hamaguchi, T. Moroi and K. Nakayama, *Flaxion: a minimal extension to solve puzzles in the standard model*, *JHEP* **01** (2017) 096 [[1612.05492](#)].
- [58] M. Millea, L. Knox and B. Fields, *New Bounds for Axions and Axion-Like Particles with KeV-GeV Masses*, *Phys. Rev. D* **92** (2015) 023010 [[1501.04097](#)].
- [59] J.L. Feng, T. Moroi, H. Murayama and E. Schnapka, *Third Generation Familons, B Factories, and Neutrino Cosmology*, *Phys. Rev. D* **57** (1998) 5875 [[hep-ph/9709411](#)].
- [60] J. Keller and A. Sedrakian, *Axions from Cooling Compact Stars*, *Nucl. Phys. A* **897** (2013) 62 [[1205.6940](#)].
- [61] A. Sedrakian, *Axion Cooling of Neutron Stars*, *Phys. Rev. D* **93** (2016) 065044 [[1512.07828](#)].
- [62] T. Fischer, S. Chakraborty, M. Giannotti, A. Mirizzi, A. Payez and A. Ringwald, *Probing Axions with the Neutrino Signal from the Next Galactic Supernova*, *Phys. Rev. D* **94** (2016) 085012 [[1605.08780](#)].
- [63] M. Giannotti, I.G. Irastorza, J. Redondo, A. Ringwald and K. Saikawa, *Stellar Recipes for Axion Hunters*, *JCAP* **1710** (2017) 010 [[1708.02111](#)].
- [64] BABAR collaboration, *A search for the decay $B^+ \rightarrow K^+ \nu \bar{\nu}$* , *Phys. Rev. Lett.* **94** (2005) 101801 [[hep-ex/0411061](#)].
- [65] *Updated fits of the UTfit collaboration at <http://www.utfit.org/UTfit/>, .*
- [66] BABAR collaboration, *Search for $B \rightarrow K^{(*)} \nu \bar{\nu}$ and invisible quarkonium decays*, *Phys. Rev. D* **87** (2013) 112005 [[1303.7465](#)].
- [67] E949, E787 collaboration, *Measurement of the $K^+ \rightarrow \pi^+ \nu \nu$ branching ratio*, *Phys. Rev. D* **77** (2008) 052003 [[0709.1000](#)].